Synthetic, structural and spectroscopic studies of sterically crowded tin-chalcogen acenaphthenes

Kasun S. Athukorala Arachchige, Louise M. Diamond, Fergus R. Knight, Marie-Luise Lechner, Alexandra M. Z. Slawin and J. Derek Woollins*

EaStCHEM, School of Chemistry, University of St Andrews, St Andrews, Fife, KY16 9ST, U.K.

Supporting Information Placeholder

ABSTRACT: A series of sterically encumbered *peri*-substituted acenaphthenes have been prepared containing chalcogen and tin moieties at the close 5,6-positions (Acenap[SnPh$_3$][ER], Acenap = acenaphthene-5,6-diyl, ER = SPh (**1**), SePh (**2**), TePh (**3**), SEt (**4**); Acenap[SnPh$_2$Cl][EPh], E = S (**5**), Se (**6**); Acenap[SnBu$_2$Cl][ER], ER = SPh(**7**), SePh (**8**), SEt (**9**)). Two geminally bis(*peri*-substituted) derivatives ({Acenap[SPh$_2$]}$_2$SnX$_2$, X = Cl (**10**), Ph (**11**)) have also been prepared, along with bromo-sulfur derivative Acenap(Br)(SEt) **15**. All eleven chalcogen-tin compounds align a Sn-C$_{Ph}$/Sn-Cl bond along the mean acenaphthene plane, and position a chalcogen lone-pair in close proximity to the electropositive tin centre promoting a weakly attractive intramolecular donor−acceptor E···Sn-C$_{Ph}$/ E···Sn-Cl 3c-4e type interaction to form. The extent of E→Sn bonding was investigated by X-ray crystallography and solution-state NMR and was found to be more prevalent in triorganotin chlorides **5**-**9** in comparison with triphenyltin derivatives **1**-**4**. The increased Lewis acidity of the tin centre resulting from coordination of a highly electronegative chlorine atom was found to greatly enhance the lp(E)−σ*(Sn−Y) donor−acceptor 3c-4e type interaction, with substantially shorter E-Sn *peri*-distances observed in the solid for triorganotin chlorides **5**-**9** (~75% ∑r_{vdW}) and significant $^1J(^{119}Sn,^{77}Se)$ spin−spin coupling constants (SSCCs) observed for **6** (163 Hz) and **8** (143 Hz) compared to triphenyltin derivative **2** (68 Hz). Similar observations were observed for geminally bis(*peri*-substituted) derivatives **10** and **11**.

INTRODUCTION

Rigid polycyclic aromatic hydrocarbons naphthalene[1] and 1,2-dihydroacenaphthylene (acenaphthene)[2] provide ideal scaffolds with which to study non-covalent intramolecular interactions.[3-7] The geometric constraints imposed by a double substitution at the proximal *peri*-positions, ensures the interacting atoms are located at distances well within the sum of their van der Waals radii, with the degree of orbital overlap and the nature of the functional groups involved dictating whether the interactions are repulsive due to steric compression or attractive as a result of bond formation.[4-7] Repulsion inevitably leads to deformation of the naturally rigid naphthalene geometry through in- and out-of-plane distortions of the exocyclic *peri*-bonds or buckling of the organic framework (angular strain) and is characteristic of much larger *peri*-distances.[4-7] For example, the introduction of bulky chalcogen atoms within the bay region of tris(sulfide) **A** (Figure 1),[8] and similarly in bis(phosphines) of type **B**,[9-11] naturally increases the steric congestion across the *peri*-gap resulting in non-bonding P···P separations that are remarkably 6-13% longer than the sum of van der Waals radii, with the *peri*-distance for the former [4.072(3) Å] the largest ever reported.[12] Bis(stannanes) **C** are further examples of severely strained molecules, with repulsion imposed by the two bulky tin centers leading to equally long *peri*-separations (~92% ∑r_{vdW}).[9,13,14] In contrast, substituent effects in 5-(dichlorophosphino)-6-(diisopropylphosphino) acenaphthene **D** induce a strongly attractive donor−acceptor interaction between the two electronically disparate functional groups, leading to a notably compressed P-P bond distance of 2.257(1) Å (63% ∑r_{vdW}).[15] Tellurium 1,2-dications **E**[16] and dithiole **F**[17] have similarly short E-E bond lengths (58-68% ∑r_{vdW}) and further demonstrate the unique ability of *peri*-substituted systems to relieve steric strain and achieve a relaxed geometry via the formation of a direct bond between the *peri*-atoms.[5,18]

Under certain geometrical conditions, the presence of weakly attractive non-covalent forces has been shown to only partially counteract the effects of steric repulsion, leading to conflicting interpretations of the (non)bonding character of the *peri*-interaction in these systems and contention over whether or not the *peri*-atoms are linked by a chemical bond.[5,19-23] For example, DAN-phosphines **G** (DAN = 8-dimethylaminonaphth-1-yl), containing weaker (i.e. longer) intramolecular N→P donor-acceptor interactions have received great attention,[19-23] with a controversial debate arising surrounding the potential occurrence of hypercoordination in these species resulting from intramolecular dative bond formation.

Similar weak intramolecular donor- acceptor interactions are found to operate in systems containing pnictogen and chalcogen moieties, with distances significantly shorter than the sum of the van der Waals radii observed between the formally nonbonded *peri*-atoms.[5,7,24-29] In bis(chalcogen) systems, the onset of 3-center-4-electron (3c4e) bonding is found to be more prevalent as larger congeners are introduced,[26-29] with a Wiberg bond index
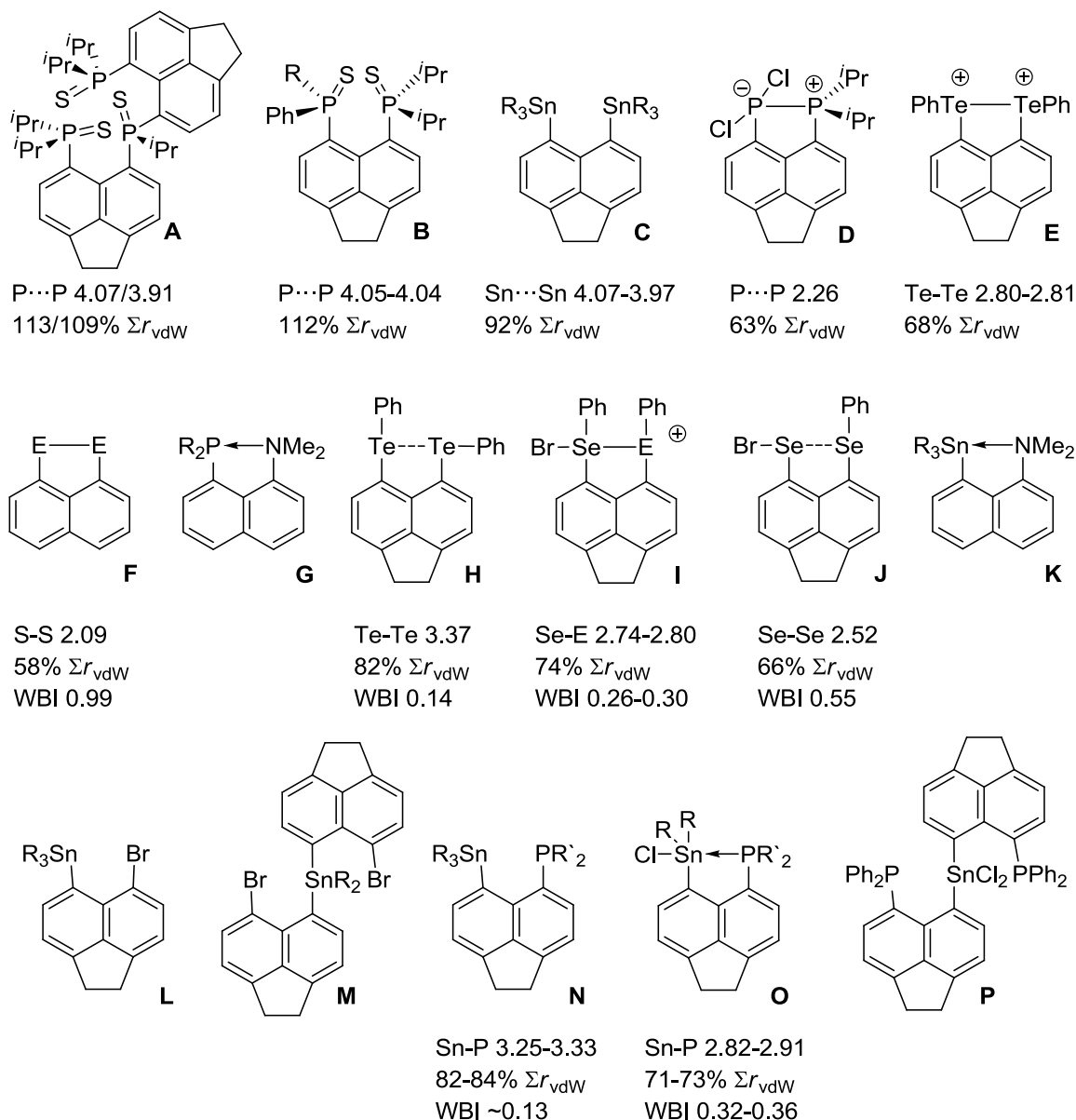
Figure 1. Heavily substituted acenaphthene and naphthalene systems characterized by non-covalent intramolecular interactions.

(WBI)[30] of 0.14 calculated for the relatively short Te⋯Te interaction (3.3674(19) Å; 82% $\sum r_{vdW}$) in 5,6-bis(phenyltelluro)acenaphthene **H** indicating a significant degree of covalent bonding.[27] In the related bromoselanyl cations **I**,[28] the presence of an additional Br atom, a good electron acceptor, shortens the Se-E distance to 74% $\sum r_{vdW}$, and is accompanied by a concomitant WBI increase to 0.26-0.30. An even stronger 3c-4e bond is predicted in **J** following the removal of a Ph group, with a WBI of 0.55 calculated for the Se-Se interaction which is anticipated to reduce to 2.52 Å (66% $\sum r_{vdW}$).[28]

In heavily substituted systems incorporating Lewis-basic groups (NR$_2$/PR$_2$) in close proximity to an electropositive tin centre (**K-P**),[31-34] a fine balance is observed between the stabilizing affects provided by the attraction of the donor/acceptor Lewis pair and the repulsive forces resulting from the steric congestion of the bay-region. During a study of sterically encumbered bromine-tin derivatives (**L, M**),[32] and more recently in a series of phosphorus-tin compounds (**N-P**),[33,34] the strength of the intramolecular Y→Sn donor-acceptor interaction was found to be highly dependent on the electronics of the substituents bound to Sn. In both

series, the extent of covalent bonding was much greater in triorganotin chlorides in comparison to their trialkyltin analogues. For instance, the increased Lewis acidity of the tin centre in triorganotin chlorides **O** naturally enhances the lp(P)−σ*(Sn−Y) donor−acceptor 3c-4e type interaction (WBI 0.32-0.36), resulting in conspicuously short P⋯Sn distances up to 29% shorter than the sum of van der Waals radii.[33] In comparison, separations in triphenyltin analogues (**N**) are notably longer (82-84% $\sum r_{vdW}$), but a significant degree of covalency is still predicted with WBIs of ~0.13 predicted for the P→Sn interaction.[33]

In this work we describe the synthesis and characterization of a series of related mixed chalcogen-tin *peri*-substituted acenaphthenes [Acenap(SnPh$_3$)(ER), Acenap = acenaphthene-5,6-diyl, ER = SPh (**1**), SePh (**2**), TePh (**3**), SEt (**4**); Acenap(SnPh$_2$Cl)(EPh), E = S (**5**), Se (**6**); Acenap(SnBu$_2$Cl)(ER), ER = SPh(**7**), SePh (**8**), SEt (**9**); {Acenap(SPh$_2$)}$_2$SnX$_2$, X = Cl (**10**), Ph (**11**); Figure 2] and investigate how the substituents bound to both the tin and chalcogen centers affect the strength of the E→Sn donor-acceptor interaction.
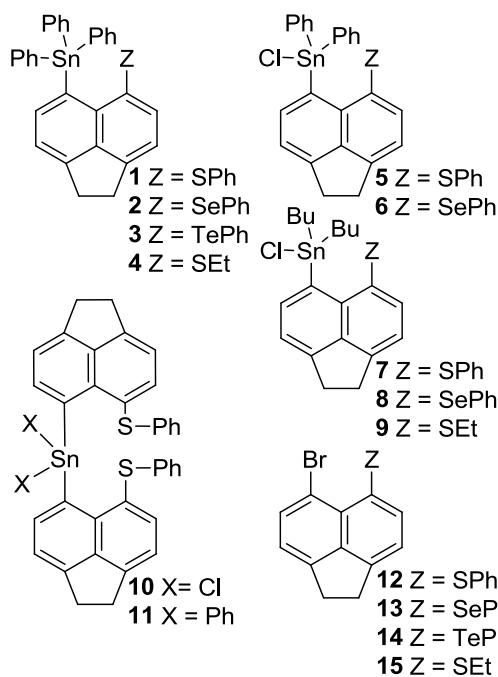
Figure 2. (6-(Organochalcogeno)acenaphth-5-yl)tin derivatives **1-11** and bromine-chalcogen precursors **12-15**.

RESULTS AND DISCUSSION

Synthesis of chalcogen-tin acenaphthene derivatives 1-11: Mixed chalcogen-tin *peri*-substituted acenaphthenes [Acenap(SnR$_3$)(ER)] **1**, **2**, **4-9** were prepared through stepwise halogen-lithium exchange reactions of previously reported 5-bromo-6-(phenylchalcogeno)acenaphthenes [Acenap(Br)(EPh)] (**12** E = S; **13** E = Se)[27] and the corresponding unknown precursor [Acenap(Br)(SEt)] (**15**) (Scheme 1). The synthesis of **15** is omitted from this manuscript, but is included in the supporting information for completeness. Crystals of **15** suitable for X-ray crystallography were grown from diffusion of hexane into a saturated solution of the product in dichloromethane; the structure of **15** and selected bond lengths and angles are deposited in the ESI.

For the synthesis of **1**, **2**, **4-9**, the respective bromine-chalcogen precursor (**12**, **13**, **15**) was treated with a single equivalent of *n*-butyllithium in diethyl ether under an oxygen- and a moisture-free nitrogen atmosphere at -78 °C, to yield *in situ* the corresponding lithium salt [Acenap(Li)(ER)]. Without isolation, addition of the respective organotin chloride [Ph$_3$ClSn, Ph$_2$Cl$_2$Sn, Bu$_2$Cl$_2$Sn] subsequently afforded [Acenap(SnPh$_3$)(SPh)] (**1**), [Acenap(SnPh$_3$)(SePh)] (**2**), [Acenap(SnPh$_3$)(SEt)] (**4**), [Acenap(SnPh$_2$Cl)(SPh)] (**5**), [Acenap(SnPh$_2$Cl)(SePh)] (**6**), [Acenap(SnBu$_2$Cl)(SPh)] (**7**), [Acenap(SnBu$_2$Cl)(SePh)] (**8**) and [Acenap(SnBu$_2$Cl)(SEt)] (**9**) in moderate to good yield [yield: 39 (**1**), 44 (**2**), 41(**4**), 40 (**5**), 39 (**6**), 23 (**7**), 62 (**8**), 53% (**9**); Scheme 1].

Due to the preferential removal of the tellurium moiety by *n*-butyllithium,[27] the corresponding reaction of [Acenap(Br)(TePh)] **14** with Ph$_3$ClSn to form [Acenap(SnPh$_3$)(TePh)] **3** was not attempted. Instead, **3** was prepared following a similar procedure, but starting from [Acenap(Br)(SnPh$_3$)][32] and with addition of diphenyl ditelluride following the initial lithiation step [yield: 79%; Scheme 1]. In addition, similar treatment of the sulfur-lithium precursor of **12** with tin chlorides SnCl$_4$ and Ph$_2$Cl$_2$Sn afforded geminally bis(*peri*-substituted) chalcogen-tin acenaphthene derivatives [{Acenap(SPh)}$_2$SnX$_2$] **10** (X = Cl) and

Scheme 1. The preparation of chalcogen-tin acenaphthenes 1-9Acenap(SnR$_3$)(ER) (ER = SPh, SePh, SEt; R$_3$ = Ph$_3$, Ph$_2$Cl, Bu$_2$Cl).[a]
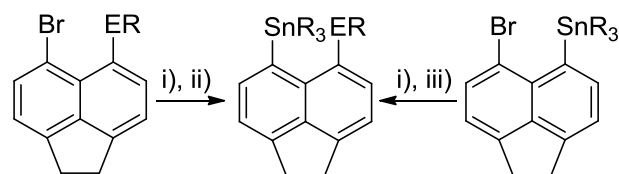
[a]Legend: (i) *n*BuLi (1 equiv.), Et$_2$O, -78 °C, 1 h; (ii) Ph$_3$ClSn (**1**, **2**, **4**)/Ph$_2$Cl$_2$Sn (**5**, **6**)/Bu$_2$Cl$_2$Sn (**7-9**) (1 equiv.), Et$_2$O, -78 °C, 30 min; r.t. 12 h; (iii) PhTeTePh (**3**) (1 equiv.), Et$_2$O, -78 °C, 30 min; r.t. 12 h.

Scheme 2. The preparation of geminally bis(*peri*-substituted) chalcogen-tin acenaphthenes 10 and 11[a]
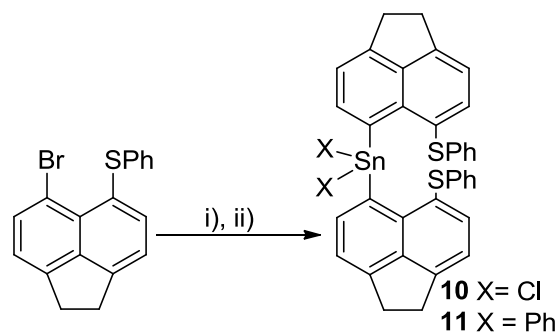
[a]Legend: (i) *n*BuLi (1 equiv.), Et$_2$O, -78 °C, 1 h; (ii) SnCl$_4$ (**10**)/Ph$_2$Cl$_2$Sn (**11**) (1 equiv.), Et$_2$O, -78 °C, 30 min; r.t. 12 h.

Table 1. ^{119}Sn, ^{77}Se and ^{125}Te NMR spectroscopy data[a].

	1	2	3	4
SnPh$_3$	**SPh**	**SePh**	**TePh**	**SEt**
δ(^{119}Sn)	-130.1	-134.8 (J_{SnSe} 68)	-146.8	-135.5
δ(^{77}Se)/δ(^{125}Te)		318	507	

	5	6
SnPh$_2$Cl	**SPh**	**SePh**
δ(^{119}Sn)	-116.9	-131.3 (J_{SnSe} 163)
δ(^{77}Se)		268

	7	8	9
SnBu$_2$Cl	**SPh**	**SePh**	**SEt**
δ(^{119}Sn)	3.56	-12.4 (J_{SnSe} 142)	-12.3
δ(^{77}Se)		271	

	10	11
SPh	**SnCl$_2$**	**SnPh$_2$**
δ(^{119}Sn)	-192.0	-166.9

[a]All spectra run in CDCl$_3$; δ values are given in ppm and J values in Hz.

11 (X = Ph), respectively [yield: 19 (**10**), 44% (**11**); Scheme 2]. All eleven compounds were characterized by multinuclear magnetic resonance spectroscopy and mass spectrometry, and the homogeneity of the new compounds was, where possible, confirmed by microanalysis. ^{119}Sn, ^{77}Se and ^{125}Te NMR spectroscopic data can be found in Table 1.

NMR investigations: The ^{119}Sn{^{1}H} NMR spectra for all eleven chalcogen-tin derivatives **1-11** display single peaks, with additional satellites observed for **2**, **6** and **8** attributed to ^{119}Sn-^{77}Se
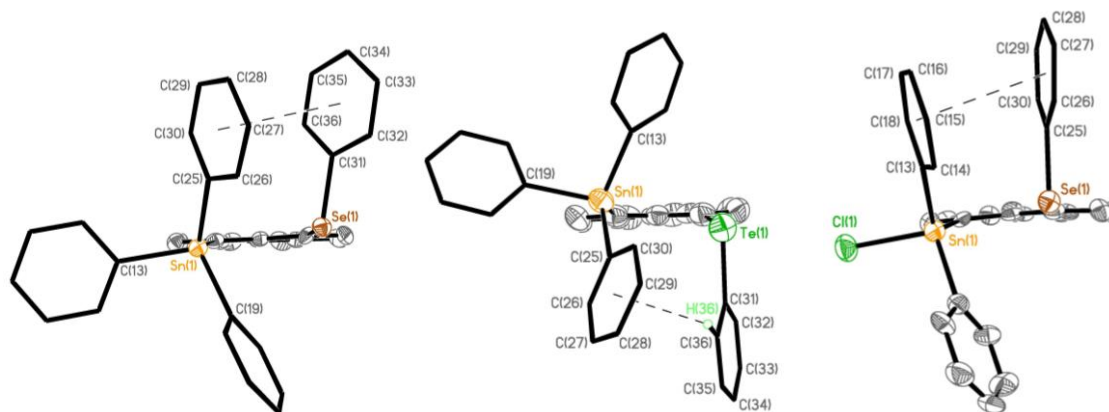
Figure 3. Molecular configurations of **2**, **3** and **6** (from left to right; 50% probability ellipsoids) showing the BCA-A (**2**, **3**) and BAA-A (**5**) type conformation of the substituents bound to Sn and E. Additional π-stacking is observed in each case, with a typical stacked arrangement in **2** and **6** and an edge-to-point arrangement in **3** due to a CH···π interaction (interacting phenyl rings are shown as wireframes and H atoms are omitted for clarity). The structures of **1** and **5**, adopting similar conformations to **2** and **6**, respectively, are omitted here but can be found in the ESI.
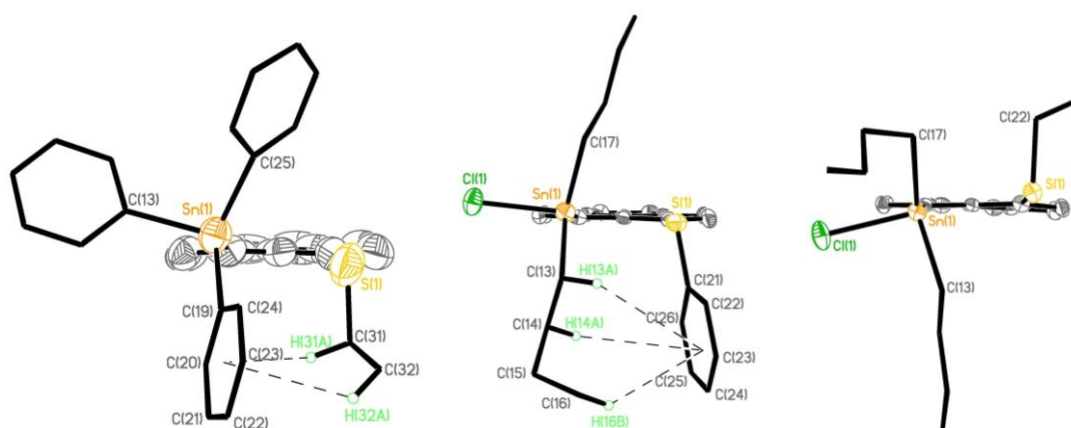

Figure 4. Molecular conformations of **4**, **7** and **9** (from left to right; 50% probability ellipsoids) showing the orientation of the *peri*-substituents (BCA-A (**4**, **9**) and BAA-A (**7**)) and weak intramolecular CH···π interactions between neighboring alkyl chains and phenyl rings in **4** and **7** (interacting phenyl rings and alkyl groups are shown as wireframes and H atoms are omitted for clarity). The structure of **8**, adopting a similar conformation to **7** is omitted here but can be found in the ESI.

coupling. Within the series of triphenyltin derivatives **1-4**, the NMR signals are consistently shifted to high field for compounds incorporating heavier chalcogen congeners (**1** SPh -130.1 ppm; **2** SePh -134.8 ppm; **3** TePh -146.8 ppm), with the exception of the SEt derivative which is shifted upfield to -135.5 ppm and comparable to the SePh analogue. A similar trend is observed for the two SnPh$_2$Cl derivatives (**5** SPh -116.9 ppm; **6** SePh -131.3 ppm) and for the corresponding SnBu$_2$Cl compounds (**7** SPh 3.6 ppm; **8** SePh -12.4 ppm; **9** SEt -12.3 ppm), with both series of triorganotin chlorides shifted notably downfield compared to their reciprocal triphenyltin analogues in accord with a reduction in electron density at the tin centre. Whilst the NMR signals for compounds **1-4** are comparable to phenyl analogue Ph$_4$Sn (-137 ppm),[35] a large upfield shift can be seen for **5** and **6** in comparison to Ph$_3$SnCl (-45 ppm),[35] consistent with the presence of an additional E···Sn interaction and a higher coordination number at the tin center. A corresponding upfield shift is observed for SnBu$_2$Cl compounds **7**, **8** and **9** in comparison to Bu$_2$PhSnCl (82.6 ppm).[36]

The relatively small $J(^{119}Sn, ^{77}Se)$ coupling observed in **2** (68 Hz) suggests only a weakly attractive through-space interaction is operating between the selenium lone-pair and the tin center in this system. In line with recently reported phosphorus-tin derivatives,[33,34] much larger $J(^{119}Sn, ^{77}Se)$ SSCCs are observed for the

triorganotin chlorides **6** (163 Hz) and **8** (142 Hz), consistent with enhanced electropositivity of the tin center following coordination to a highly electronegative chlorine atom and subsequent increase in the strength of the donor-acceptor through-space Se→Sn lone-pair interaction. The reciprocal $^{77}Se\{^1H\}$ NMR spectra for **2**, **6** and **8** appear as anticipated singlets accompanied by satellites for ^{119}Sn-^{77}Se coupling, with J_{SeSn} values correlating to those observed in the $^{119}Sn\{^1H\}$ NMR spectra. As expected, the signals move to low field on going from triphenyltin derivative **2** (δ_{Se} 318 ppm) to triorganotin chlorides **6** (δ_{Se} 268 ppm) and **8** (δ_{Se} 271 ppm). The $^{119}Sn\{^1H\}$ NMR spectra for geminally bis(*peri*-substituted) systems **10** and **11** display single peaks, with the signal for the chlorine analogue lying upfield (δ_{Sn} -192.0 ppm) compared to the phenyl derivative (δ_{Sn} -166.9 ppm).

X-ray investigations. Suitable single crystals were obtained for **1-3**, **5-8**, **10** and **11** from recrystallisation by diffusion of hexane into a saturated solution of the compound in THF. Crystals for **9** were obtained by recrystallisation from a saturated solution of the compound in THF at -30 °C and for **4** and **15** from diffusion of hexane into a saturated solution of the compound in DCM. All compounds crystallize with one molecule in the asymmetric unit except for **5** which contains two independent molecules which are

Table 2. Selected interatomic distances [Å] and angles [°] for Acenap[SnPh₃][ER] compounds 1-4.

Compound	1	2	3	4
SnR₃/ER	SnPh₃/SPh	SnPh₃/SePh	SnPh₃/TePh	SnPh₃/SEt
Peri-region-distances				
Sn(1)···E(1)	3.271(2)	3.341(1)	3.490(1)	3.221(2)
Σr$_{vdW}$ - Sn···E[a]	0.699	0.729	0.740	0.749
% Sr$_{vdW}$[a]	82	82	83	81
Sn(1)-C(1)	2.156(5)	2.171(6)	2.166(5)	2.147(4)
E(1)-C(9)	1.792(5)	1.932(6)	2.106(6)	1.781(7)
Peri-region bond angles				
Sn(1)-C(1)-C(10)	127.0(4)	128.1(4)	127.9(5)	126.3(3)
C(1)-C(10)-C(9)	129.0(4)	128.8(5)	129.9(5)	128.7(5)
E(1)-C(9)-C(10)	121.7(4)	123.2(4)	122.9(4)	121.4(4)
Σ of bay angles	**377.7(7)**	**380.1(8)**	**380.7(8)**	**376.4(7)**
Splay angle[b]	17.7	20.1	20.7	16.4
C(4)-C(5)-C(6)	111.9(5)	112.0(5)	112.2(5)	112.4(7)
Out-of-plane displacement				
Sn(1)	0.289	-0.250	0.456	0.499
E(1)	-0.183	0.200	-0.468	-0.255
Central naphthalene ring torsion angles				
C:(6)-(5)-(10)-(1)	179.0(4)	-179.0(5)	175.7(6)	177.4(5)
C:(4)-(5)-(10)-(9)	176.3(4)	-177.4(5)	177.9(6)	175.9(4)

[a] van der Waals radii used for calculations: r$_{vdW}$(Sn) 2.17 Å, r$_{vdW}$(S) 1.80 Å; r$_{vdW}$(Se) 1.90 Å; r$_{vdW}$(Te) 2.06 Å; [b] Splay angle: Σ of the three bay region angles – 360.

Table 3. Selected interatomic distances [Å] and angles [°] for Acenap[SnR₂Cl][ER] compounds 5-9.

Compound	5	6	7	8	9
SnR₂Cl/ER	SnPh₂Cl/SPh	SnPh₂Cl/SePh	SnBu₂Cl/SPh	SnBu₂Cl/SePh	SnBu₂Cl/SEt
Peri-region-distances					
Sn(1)···E(1)	2.979(2) [2.989(2)]	3.093(2)	2.982(1)	3.059(1)	2.982(2)
Σr$_{vdW}$ - Sn···E[a]	0.991 [0.981]	0.976	0.988	1.011	0.988
% Sr$_{vdW}$[a]	75 [75]	76	75	75	75
Sn(1)-C(1)	2.136(6) [2.143(5)]	2.158(10)	2.168(3)	2.170(7)	2.164(4)
E(1)-C(9)	1.765(6) [1.777(5)]	1.926(11)	1.775(4)	1.920(7)	1.785(4)
Sn(1)-Cl(1)	2.464(1) [2.484(1)]	2.423(4)	2.463(1)	2.494(2)	2.456(2)
Peri-region bond angles					
Sn(1)-C(1)-C(10)	123.9(4) [122.0(3)]	122.9(8)	122.3(3)	123.0(5)	121.7(4)
C(1)-C(10)-C(9)	126.9(5) [128.8(5)]	128.7(10)	128.6(3)	130.3(6)	127.9(4)
E(1)-C(9)-C(10)	120.1(5) [120.5(4)]	121.0(8)	119.9(3)	119.4(5)	120.2(4)
Σ of bay angles	**370.9(8) [371.3(7)]**	**372.6(15)**	**370.8(5)**	**372.7(9)**	**369.8(7)**
Splay angle[b]	10.9 [11.3]	12.6	10.8	12.7	9.8
C(4)-C(5)-C(6)	112.9(6) [111.6(5)]	113.8(10)	112.0(3)	112.3(6)	112.0(4)
Out-of-plane displacement					
Sn(1)	-0.279 [-0.154]	-0.263	0.234	0.207	-0.229
E(1)	-0.112 [0.013]	0.331	-0.027	-0.015	0.342
Central naphthalene ring torsion angles					
C:(6)-(5)-(10)-(1)	-179.8(5) [-175.6(4)]	-176.6(7)	177.8(3)	177.8(6)	-176.0(4)
C:(4)-(5)-(10)-(9)	178.5(5) [-178.1(4)]	-178.5(7)	-179.8(3)	179.7(6)	-177.1(4)

[a] van der Waals radii used for calculations: r$_{vdW}$(Sn) 2.17 Å, r$_{vdW}$(S) 1.80 Å; r$_{vdW}$(Se) 1.90 Å; r$_{vdW}$(Te) 2.06 Å; [b] Splay angle: Σ of the three bay region angles – 360.

Table 4. Selected interatomic distances [Å] and angles [°] for [{Acenap(SPh)}$_2$(SnR$_2$)] compounds 10 and 11.

Compound	10		11	
SnR$_3$/ER	SnCl$_2$/SPh	SnCl$_2$/SPh	SnPh$_2$/SPh	SnPh$_2$/SPh
Peri-region-distances				
Sn(1)···S(1)	2.937(2)	2.970(2)	3.281(1)	3.230(1)
Σr_{vdW} - Sn···S[a]	1.03	1.00	0.789	0.840
% Sr$_{vdW}$[a]	74	75	81	79
Sn(1)-C(1)	2.140(6)	2.132(7)	2.172(3)	2.172(3)
S(1)-C(9)	1.778(7)	1.777(7)	1.782(4)	1.785(4)
Sn(1)-Cl(1)	2.4104(18)	2.4194(19)		
Peri-region bond angles				
Sn(1)-C(1)-C(10)	121.2(5)	121.3(5)	126.7(3)	127.4(3)
C(1)-C(10)-C(9)	129.1(6)	129.7(6)	128.6(3)	129.3(3)
S(1)-C(9)-C(10)	118.8(5)	119.0(5)	121.8(3)	120.2(3)
Σ of bay angles	**369.1(9)**	**370.0(9)**	**377.1(5)**	**376.9(5)**
Splay angle[b]	9.1	10.0	17.1	16.9
C(4)-C(5)-C(6)	113.0(6)	112.4(6)	111.5(3)	111.8(3)
Out-of-plane displacement				
Sn(1)	-0.175	-0.219	0.493	-0.320
S(1)	-0.214	-0.015	-0.262	-0.037
Central naphthalene ring torsion angles				
C:(6)-(5)-(10)-(1)	179.3(5)	-179.9(6)	173.4(3)	-178.9(3)
C:(4)-(5)-(10)-(9)	-178.4(5)	-179.6(6)	178.6(3)	179.0(3)

[a] van der Waals radii used for calculations: r_{vdW}(Sn) 2.17 Å, r_{vdW}(S) 1.80 Å; [b] Splay angle: Σ of the three bay region angles – 360.

Table 5. Bond angles [°] categorizing the geometry around Sn in 1-9.

	1	2	3	4
C(1)-Sn(1)-C(13)	104.45(18)	105.2(2)	110.1(3)	102.80(17)
C(1)-Sn(1)-C(19)	115.37(17)	111.4(2)	105.2(3)	116.22(17)
C(1)-Sn(1)-C(25)	111.48(18)	115.1(2)	121.1(3)	114.38(18)
C(13)-Sn(1)-C(19)	104.93(18)	104.2(2)	100.9(3)	105.24(18)
C(13)-Sn(1)-C(25)	105.13(18)	104.0(2)	113.6(3)	100.26(18)
C(19)-Sn(1)-C(25)	114.17(18)	115.4(2)	103.2(3)	115.14(18)

	5	6		7	8	9
C(1)-Sn(1)-C(13)	118.5(2) [118.5(2)]	120.7(4)	C(1)-Sn(1)-C(13)	123.83(14)	113.7(3)	115.44(17)
C(1)-Sn(1)-C(19)	115.9(2) [115.11(19)]	113.4(4)	C(1)-Sn(1)-C(17)	114.16 (13)	122.6(3)	118.18(19)
C(1)-Sn(1)-Cl(1)	99.82(15) [98.05(14)]	99.7(3)	C(1)-Sn(1)-Cl(1)	96.77(9)	96.89(18)	96.73(15)
C(1)-Sn(1)-E(1)	75.53(15) [76.70(14)]	77.4(3)	C(1)-Sn(1)-E(1)	75.78(9)	77.24(17)	76.05(15)
C(13)-Sn(1)-C(19)	119.9(2) [119.43(19)]	117.8(4)	C(13)-Sn(1)-C(17)	118.30(14)	120.5(3)	122.79(18)
C(13)-Sn(1)-Cl(1)	95.92(16) [82.02(15)]	97.9(3)	C(13)-Sn(1)-Cl(1)	94.34(10)	97.6(3)	93.64(17)
C(13)-Sn(1)-E(1)	88.09(16) [98.43(15)]	80.8(3)	C(13)-Sn(1)-E(1)	90.94(10)	84.6(2)	85.75(18)
C(19)-Sn(1)-Cl(1)	98.18(15) [100.01(16)]	101.1(4)	C(17)-Sn(1)-Cl(1)	98.33(10)	93.5(2)	98.51(17)
C(19)-Sn(1)-E(1)	82.35(15) [84.73(16)]	83.3(3)	C(17)-Sn(1)-E(1)	83.85(10)	90.03(19)	88.85(18)

chemically identical, but differ slightly crystallographically and **10** which crystallizes with one molecule of THF and one molecule of cyclohexane per molecule of product. In addition, the structure of **9** contains one disordered CH$_3$ group over symmetry elements and is refined with half occupancy. Selected interatomic bond lengths and angles are given in Tables 2−6. Further crystallographic information can be found in the Supporting Information.

In the solid, the series of triphenyltin derivatives **1**-**4**, diphenyltin chlorides **5** and **6**, and the corresponding dibutyltin chlorides **7**-**9** all adopt similar molecular configurations, categorised according to the classification system devised by Nakanishi *et al.*[7] and Nagy *et al.*[37] as type BCA-A (**1-4**, **6** and **9**) and BAA-A (**5**, **7** and **8**) (Figures 3 and 4; S2, S4, S6, ESI). In each case, two Sn-C$_R$ bonds align roughly perpendicular to the acenaphthene
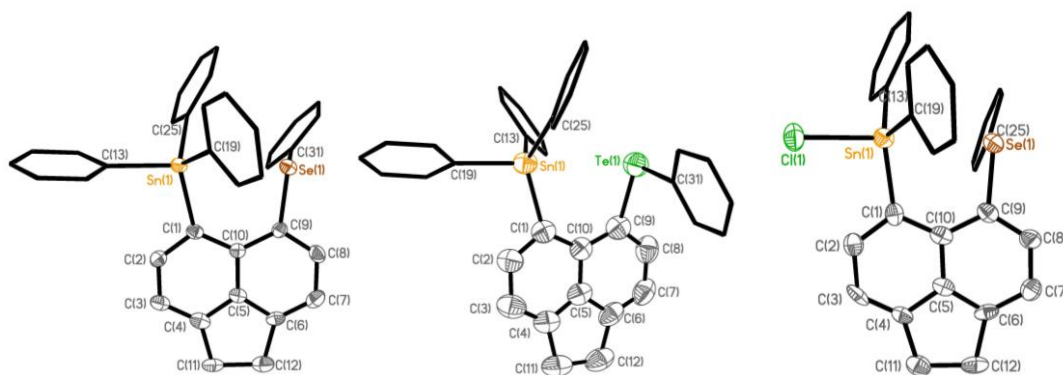
Figure 5. Molecular structures of **2**, **3** and **6** (from left to right; 50% probability ellipsoids; phenyl rings are shown as wireframes and H atoms are omitted for clarity). The structures of **1** and **5**, adopting similar conformations to **2** and **6**, respectively, are omitted here but can be found in the ESI.
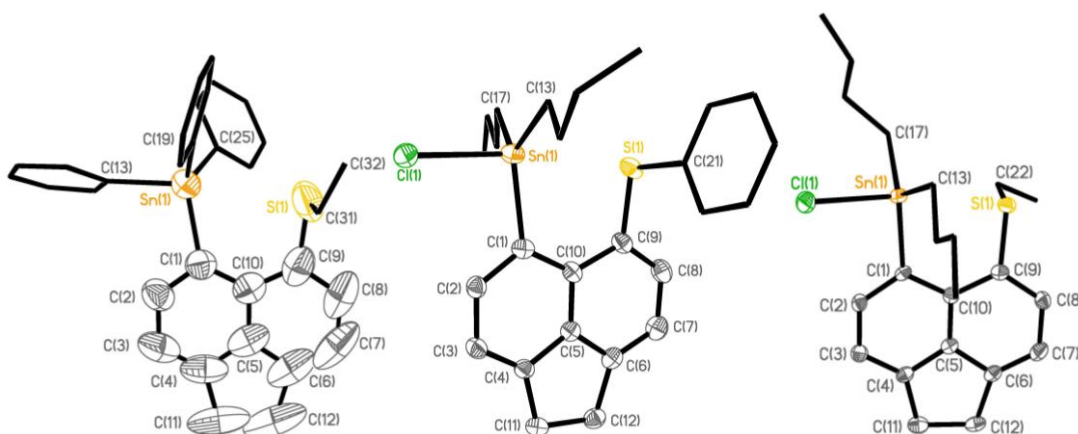

Figure 6. Molecular structures of **4**, **7** and **9** (from left to right; 50% probability ellipsoids; phenyl rings and alkyl groups are shown as wireframes and H atoms are omitted for clarity). The structure of **8**, adopting a similar conformation to **7** is omitted here but can be found in the ESI.

backbone, adopting comparable axial (type A) or twist (type C) conformations, and displacing the alkyl moieties to opposite sides of the molecule. The coplanar location of the remaining Sn-C$_{Ph}$ bonds in **1**-**4** and a similar equatorial alignment of the Sn-Cl bonds in **5**-**9** (type B), gives rise to *quasi*-linear C$_{Ph}$-Sn···E and Cl-Sn-E three-body fragments, respectively, in which angles approach 180° (172-179°).

In compounds **1**-**8**, a reciprocal perpendicular alignment of the E-C$_R$ bond at the second *peri*-position across the bay, positions the E(alkyl) substituent in close proximity to one of the alkyl substituents on the tin centre. In triphenyltin analogues **1** (S(phenyl)) and **2** (Se(phenyl)), the two axial phenyl rings are twisted to align non-planar/non-perpendicular (np) with respect to the acenaphthene ring (Figure S6, ESI),[7] but their parallel arrangement still allows for a significant overlap of the π-systems, with centroid-centroid distances (**1** Cg(19-24)···Cg(31-36) 3.77 Å; **2** Cg(25-30)···Cg(31-36) 3.80 Å) in both cases in the correct range for π-π stacking (3.3-3.8 Å;[38] Figures 3 and S2). A similar arrangement is observed in diphenyltin chlorides **5** and **6**, which exhibit centroid-centroid distances of 3.73 Å (**5** Cg(13-18)···Cg(25-30)) and 3.82 Å (**6** Cg(13-18)···Cg(25-30); Figures 3 and S2). In contrast, the corresponding phenyl rings in the heavier Te(phenyl) analogue **3** no longer align parallel, but instead interact with a distorted edge-to-face arrangement (T-shaped) resulting from the presence of a C-H···π interaction (H36···Cg(25-30) 2.89 Å; Figure 3).[39] Comparable weak intramolecular interactions are also present in S(ethyl) analogue **4**, and dibutyltin chlorides **7** and **8**, with C-H···π interac-

tions linking an alkyl chain to an adjacent phenyl ring in each case (**4** H31A···Cg(19-24) 3.38 Å, H32A···Cg(19-24) 3.15 Å; **7** H13A···Cg(21-26) 3.35 Å, H14A···Cg(21-26) 3.22 Å, H16B···Cg(21-26) 3.24 Å; **8** H17A···Cg(21-26) 3.55 Å, H18A···Cg(21-26) 3.34 Å, H20B···Cg(21-26) 3.13 Å; Figures 4 and S4). No equivalent interactions are observed in compound **9**, despite the ethyl and butyl substituents lying in close proximity as a result of an axial-axial pairing (Figure 4).

Nevertheless, the predominant factor dictating the final solid-state structure of all nine compounds is the nature of the nonbonded interactions that arise in the *quasi*-linear C$_{Ph}$-Sn···E and Cl-Sn-E three-body fragments, due to the direct overlap of the closely located and linearly aligned orbitals. In these systems, steric repulsion between the bulky chalcogen and tin moieties is counterbalanced by the presence of a weakly attractive donor-acceptor 3c-4e type interaction, resulting from the delocalisation of a chalcogen lone-pair to an antibonding σ*(Sn-C$_{Ph}$) orbital. The strength of the Sn···E interaction is subsequently influenced by the degree of orbital overlap in these systems and thus the size of the interacting atoms, although the sterics and electronics of the substituents bound to the *peri*-atoms also play an important role in controlling their fine structures.

In line with related bis(chalcogen) systems,[26-28] substitution of increasingly large functional groups at the close contact *peri*-positions in triphenyltin derivatives **1**-**4** increases the steric pressure within the bay-region and leads to greater deformation of the natural acenaphthene geometry (Figures 5 and 6). Non-bonded

peri-distances [**1** 3.271(2) Å; **2** 3.413(12) Å; **3** 3.490(1) Å] and corresponding splay angles [**1** 17.1°; **2** 20.1°; **3** 20.7°] increase steadily as heavier congeners of Group 16 are located at the proximal 5,6-positions, whilst replacement of the S(phenyl) moiety in **1** with a less bulky S(ethyl) group in **4** results in an expected decrease in molecular strain [**4** 3.221(2) Å, 16.4°]. Despite this, nonbonded Sn···E *peri*-distances in all four derivatives are ~18% shorter than the sum of the respective van der Waals radii and a significant degree of covalency is predicted between Sn and E in each case. For comparison, the corresponding C_{Ph}-Sn···P three-body fragment found in the related phosphorus-tin analogue [Acenap(SnPh$_3$)(P^{i}Pr$_2$)], in which the Sn···P distance is similarly 18% shorter than the sum of van der Waals radii, was found to contain significant 3c-4e character, with a Wiberg bond index (WBI) of 0.12 having been computed for the Sn···P interaction.[33]

Similar to related phosphorus-tin compounds,[33,34] replacement of an equatorial phenyl group with a highly electronegative chlorine atom in diphenyltin chlorides **5** and **6** is accompanied by a dramatic reduction in the length of the two Sn···E *peri*-distances [**5** 2.979(2) Å [2.989(2) Å]; **6** 3.094(2) Å; *cf.* **1** 3.271(2) Å; **2** 3.413(12) Å]. Dibutyltin chlorides **7-9** display equally short intramolecular Sn···E distances [**7** 2.982(1) Å; **8** 3.059(1) Å; **9** 2.982(2) Å], and for all five tin chlorides these separations are ~25% shorter than the sum of van der Waals radii and approach the distance for single electron pair (2c-2e) Sn-S (2.51 Å) and Sn-Se (2.59 Å) covalent bonds.[12] As such, much stronger multicentre bonding is predicted to occur in **5-9** as a consequence of the increased Lewis-acidity at the tin centre, explaining the notable increase in $J(^{119}Sn,^{77}Se)$ through-space coupling observed in chlorides **6** (163 Hz) and **8** (142 Hz) compared to **2** (68 Hz). This is consistent with the findings from previous studies of phosphorus-tin compounds,[33,34] where substantial WBIs of up to 0.36 were calculated for a series of analogous triorganotin chlorides in which the Sn-P *peri*-distances were also notably compressed (72% $\sum r_{vdW}$).[33] The presence of a hypervalent 3c-4e type interaction operating in **5-9** is further supported by the natural reduction in the Sn-Cl bond order observed following donation of the chalcogen lone-pair into the σ*(Sn-Cl) orbital, with the equatorial Sn-Cl bond in each case becoming weaker and longer than in the corresponding triorganotin chloride starting material [**5** 2.4639(14) Å [2.4836(13) Å]; **6** 2.423(4) Å; **7** 2.4635(11) Å; **8** 2.494(2) Å; **9** 2.4557(18) Å; *cf.* Ph$_3$SnCl 2.12 Å; Ph$_2$SnCl$_2$ 2.373(9) Å; Bu$_2$SnCl$_2$ 2.413 Å].[40]

As expected, the stronger 3c-4e Cl-Sn-E bonding present in **5-9** has a greater impact on counteracting the steric repulsion that invariably builds up between the closely aligned Sn and E lone-pair orbitals and is thus accompanied by a substantial reduction in molecular distortion. This is most apparent within the acenaphthene plane where the divergence of the exocyclic Sn- C_{Acenap} and E-C_{Acenap} bonds is notably less pronounced [splay angles **5** 10.9°[11.3°]; **6** 12.6°; **7** 10.8°; **8** 12.7°; **9** 9.8°] than in the triphenyltin derivatives **1-4** [splay angles 16-21°] (Figures 5 and 6).

In the series of triphenyltin derivatives **1-4**, the bulk of the aromatic rings coupled with the presence of the additional intramolecular Sn···E interaction forces the central tin atom to adopt a distorted tetrahedral geometry. C–Sn–C angles lie in the range 99.64(14)°-120.86(15)° and for each tin centre the three pseudo-equatorial C-Sn-C bond angles sum to 341-346° (Table 5), intermediate between an ideal tetrahedron (328.5°) and a perfect trigonal bipyramid (360°). The increased strength of the Sn-E interaction in **5-9** causes even greater distortion to the naturally tetrahedral tin environment, with the sum of the pseudo-equatorial C-Sn-C angles increasing to between 353-357°, more in line with a trigonal bipyramidal geometry (Table 5). This is supported by looking at the geometrical goodness [$\Delta\sum(\theta) = \Delta\sum(\theta_{eq}) - \Delta\sum(\theta_{ax})$; 0° (tetrahedron) $\leq \Delta\sum(\theta) \leq$ 90° (trigonal bipyramid)][34] for each

compound, which steadily increases from $\Delta\sum(\theta) = 26.5°$ (**1**), 28.5° (**2**), 35.5° (**3**), 37.4° (**4**) in the triphenyltin derivatives to $\Delta\sum(\theta) = 60.4°[72.7°]$ (**5**), 53.2° (**6**), 66.9°(**7**), 68.8° (**8**), 67.5° (**9**) in the triorganotin chlorides.

The molecular structure of bis(*peri*-substituted) sulfur-tin acenaphthene [{Acenap(SPh)}$_2$SnCl$_2$] **10** is constructed from two crystallographically unique acenaphthene fragments which couple through a central *pseudo*-hexacoordinated tin atom in a geminal fashion (Figure 7). The molecule crystallizes in a conformation which fixes the sulfur atoms and the tin centre in close proximity, forming a relatively compact triangular S$_2$Sn cluster [S1-Sn1-S21 85.33(5)°, Sn1-S1-S21 47.68(4)°, Sn1-S21-S1 46.99(4)°]. The two equally compressed Sn···S *peri*-distances [Sn1-S1 2.9368(19) Å, Sn1-S21 2.9698(19) Å] are significantly shorter than the sum of van der Waals radii (~74% $\sum r_{vdW}$), and result from strong lp(S)−σ*(Sn−Cl) donor-acceptor interactions operating between the closely located sulfur lone-pairs and the electropositive Sn atom. Coordination of two highly electronegative chlorine atoms naturally increases the Lewis acidity of the tin centre compared to monosystems **5**, **7** and **9**, leading to marginally shorter distances and stronger multicentre bonding. The perpendicular and coplanar alignment of the two acenaphthene scaffolds (Figure 8), which lie with an angle of 88° between the two mean planes, also results in a relatively short intramolecular S···S distance of 4.003(2) Å and an S1-Sn-S21 angle of 85.33(5)°.

In each acenaphthene fragment, the S(phenyl) moiety and one of the chlorine atoms adopt axial positions, with the S-C_{Ph} and Sn-Cl bonds aligning perpendicular to the mean plane of the organic backbone (type A). In the first fragment the two groups are displaced to opposite sides of the acenaphthene plane (type AA*t*),[7,37] whilst in the second they are *cis* disposed (type AA*c*).[7,37] Each Sn-Cl bond subsequently aligns coplanar with the neighboring acenaphthene backbone (type B),[7,37] giving rise to a *quasi*-linear Cl-Sn···S three-body fragment, in which angles approach 180° [S1-Sn1-Cl2 175.63(6)°, S21-Sn1-Cl1 170.97(6)°](Figure 8).

The bonding around the tin centre in dichloride **10** (Table 6) is somewhat more complex and intriguing than that observed in **1-9**, with the geometry at the metal centre best described as either 2-coordinate (linear), 4-coordinate (see-saw) or 6-coordinate (octahedral) depending upon the interpretation of the bonding situation. In the former, the weakly attractive S-Sn lone-pair interaction is classed as non-bonding, whilst the nature of the Sn-Cl bond is ascribed as ionic due to the substantial disparity between the electronegativities of the Sn and Cl atoms. This leaves the tin centre coordinated to two carbon atoms, one from each of the coupling acenaphthene backbones, with a C-Sn-C bond angle of 151.4(3)°. Alternatively, the two Sn-Cl bonds can be thought to retain enough covalent character as to describe the geometry as distorted disphenoidal (see-saw), similar to the related tin-bromine dichloride derivative {AcenapBr}$_2$SnCl$_2$,[32] and with the four C-Sn-Cl bond angles summing to 397°. The two additional intramolecular S→Sn lone-pair interactions, which complete a *quasi*-octahedral geometry around the tin centre, thus play an important role in determining the overall conformation of the metal. S1 and S21 occupy two equatorial positions with standard deviation from the mean Sn1-Cl1-Cl2-S1-S21 plane only 0.0271 Å. Similar to tin chlorides **5-9**, the effect of the two S→Sn lone-pair interactions is to naturally lower the covalency of the two Sn–Cl bonds, which are longer and weaker (2.4104(18) Å, 2.4194(19) Å) than equivalent bonds in related Ar$_2$SnCl$_2$ compounds {AcenapBr}$_2$SnCl$_2$ (2.379(3) Å, 2.390(3) Å)[32] and SnPh$_2$Cl$_2$ (2.373(9) Å).[40]
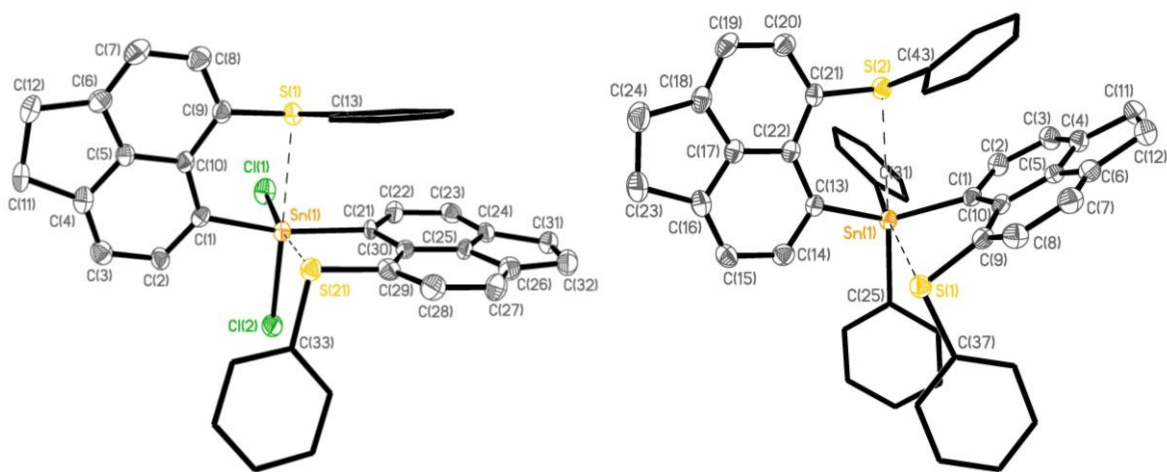
Figure 7. Molecular structures of **10** and **11** (50% probability ellipsoids; phenyl rings are shown as wireframes and H atoms are omitted for clarity). The co-crystallized THF and cyclohexane molecules in **10** are also omitted.
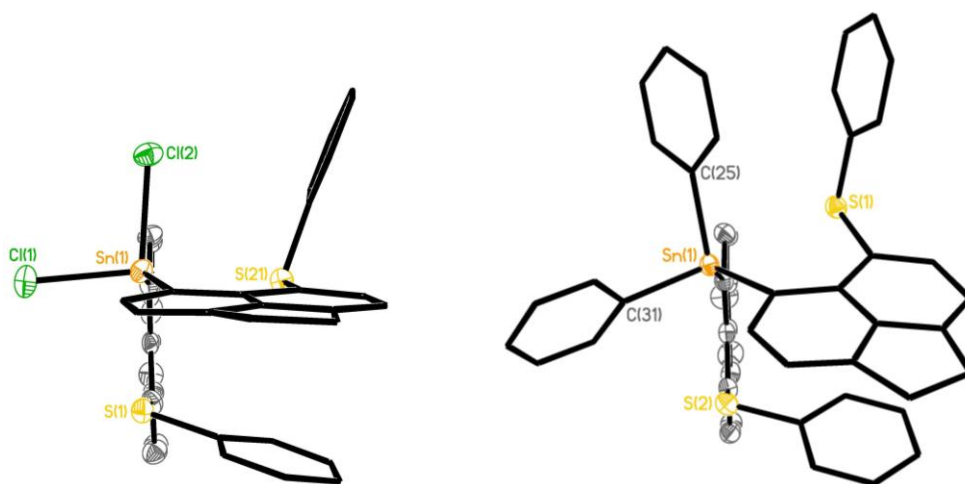

Figure 8. Molecular configurations of **10** and **11** (50% probability ellipsoids) showing the conformation of the *peri*-substituents (phenyl rings and one acenaphthene group are shown as wireframes and H atoms are omitted for clarity).

Table 6. Bond angles [°] categorizing the geometry around Sn in 10 and 11.

	10		**11**
Cl(1)-Sn(1)-Cl(2)	98.32(7)	**C(25)-Sn(1)-C(31)**	99.82(11)
Cl(1)-Sn(1)-S(1)	85.72(6)	**C(25)-Sn(1)-S(1)**	77.96(8)
Cl(1)-Sn(1)-C(1)	98.49(17)	**C(25)-Sn(1)-C(1)**	107.76(12)
Cl(1)-Sn(1)-C(21)	100.88(19)	**C(25)-Sn(1)-C(13)**	108.79(12)
Cl(1)-Sn(1)-S(21)	170.97(6)	**C(25)-Sn(1)-S(2)**	176.40(8)
Cl(2)-Sn(1)-S(1)	175.63(6)	**C(31)-Sn(1)-S(1)**	175.16(10)
Cl(2)-Sn(1)-C(1)	100.53(19)	**C(31)-Sn(1)-C(1)**	105.95(12)
Cl(2)-Sn(1)-C(21)	97.25(19)	**C(31)-Sn(1)-C(13)**	109.55(12)
Cl(2)-Sn(1)-S(21)	90.66(6)	**C(31)-Sn(1)-S(2)**	76.85(10)
S(1)-Sn(1)-C(1)	77.13(19)	**S(1)-Sn(1)-C(1)**	70.95(10)
S(1)-Sn(1)-C(21)	83.55(19)	**S(1)-Sn(1)-C(13)**	75.27(9)
S(1)-Sn(1)-S(21)	85.33(5)	**S(1)-Sn(1)-S(2)**	105.46(2)
C(1)-Sn(1)-C(21)	151.4(3)	**C(1)-Sn(1)-C(13)**	122.59(11)
C(1)-Sn(1)-S(21)	80.69(19)	**C(1)-Sn(1)-S(2)**	74.68(10)
C(21)-Sn(1)-S(21)	76.90(18)	**C(13)-Sn(1)-S(2)**	71.43(10)

Diphenyltin analogue [{Acenap(SPh)}$_2$SnPh$_2$] **11** adopts a comparable molecular structure to that of dichloride **10**, with two crystallographically distinct acenaphthene backbones coupling through a central tin atom to form a geminally bis(*peri*-substituted) system (Figure 7). Nevertheless, notable changes are observed between the two structures upon replacing the two highly electronegative chlorine atoms in **10** with two bulky phenyl groups in **11**.

Within the triangular S$_2$Sn cluster [S1-Sn1-S2 105.46(2)°, Sn1-S1-S2 36.930(17)°, Sn1-S2-S1 37.608(16)°], the S···Sn distances [Sn1-S1 3.2807(14) Å; Sn1-S2 3.2300(13) Å] are notably longer, indicative of much weaker lp(S)−σ*(Sn−Cl) donor-acceptor interactions and a natural reduction in the Lewis acidity of the tin centre. Nonetheless, these separations are still 17-19% shorter than the sum of van der Waals radii for S/Sn (3.97 Å) and a significant 3c-4e interaction is still predicted to be present, similar in strength to the interactions in triphenyltin analogues **1** and **4**. A non-perpendicular and non-coplanar alignment of the two acenaphthene backbones in **11** (Figure 8), further increases the size of the triangular cluster, with the S1-Sn-S2 angle increasing to 105.46(2)° [*cf.* **10** 85.33(5)°] resulting in a nonbonded S···S distance of 5.1815(18) Å [*cf.* **10** 4.003(2) Å]. Despite these differ-

ences, the arrangement of the *peri*-substituents in the two acenaphthene fragments is comparable to dichloride **10**, with a mutual axial-axial pairing of S(phenyl) and Sn(phenyl) moieties, resulting in two *quasi*-linear C_{Ph}-Sn⋯S three-body fragment from the equatorial alignment of each Sn-C_{Ph} bond with the neighboring acenaphthene backbone [S1-Sn1-C31 175.16(10)°, S2-Sn1-C25 176.40(8)°]. With much weaker S⋯Sn interactions operating in **11**, the geometry around the tin centre moves closer towards a natural tetrahedron, with angles in the range 99.82(11)-122.59(11)° and summing to 109°. The more acute C1-Sn1-C13 angle of 122.59(11)° in **11** compared to 151.4(3)° for the reciprocal C1-Sn1-C21 angle in **10** illustrates the degree to which the alignment of the two acenaphthene backbones differs in the two compounds.

CONCLUSION

Sterically encumbered *peri*-substituted acenaphthenes [Acenap(SnPh₃)(ER), Acenap = acenaphthene-5,6-diyl, ER = SPh (**1**), SePh (**2**), TePh (**3**), SEt (**4**); Acenap(SnPh₂Cl)(EPh), E = S (**5**), Se (**6**); Acenap(SnBu₂Cl)(ER), ER = SPh(**7**), SePh (**8**), SEt (**9**); {Acenap(SPh₂)}₂SnX₂, X = Cl (**10**), Ph (**11**)] have been prepared from standard halogen-lithium exchange reactions of [Acenap(Br)(SPh)] **12**,[27] [Acenap(Br)(SePh)] **13**,[27] [Acenap(Br)(SnPh₃)][32] and [Acenap(Br)(SEt)] **15**. X-ray structures were determined for **1-11** (and **15**) and have been used in conjunction with ⁷⁷Se{¹H} and ¹¹⁹Sn{¹H} NMR spectroscopy to investigate how the sterics and electronics of substituents bound to tin affect the strength of the intramolecular lp(P)−σ*(Sn−Y) donor−acceptor 3c-4e type interactions operating in these systems.

The series of triphenyltin derivatives **1-4**, diphenyltin chlorides **5** and **6**, and the corresponding dibutyltin chlorides **7-9** adopt similar conformations, categorized as type BCA-A (**1-4**, **6** and **9**) and BAA-A (**5**, **7** and **8**).[7,37] In both arrangements two Sn-C_R bonds align roughly perpendicular to the mean acenaphthene plane but on opposing sides of the molecule (axial type A or twist type C configurations),[7,37] with the remaining Sn-C_{Ph} (**1-4**) and Sn-Cl (**5-9**) bonds occupying positions along the acenaphthene backbone (type B)[7,37] giving rise to *quasi*-linear C_{Ph}-Sn⋯E and Cl-Sn-E three-body fragments, respectively.

The geometric constraints imposed by the acenaphthene backbone and the linear alignment of the orbitals in these systems provides the correct geometrical environment to promote delocalization of the chalcogen lone-pair to an antibonding σ*(Sn−Y) orbital to form a donor−acceptor three-centre−four-electron (3c-4e) type interaction.

Within the series of triphenyltin derivatives, molecular distortion steadily increases as larger chalcogen congeners occupy the *peri*-space, with *peri*-distances increasing from 3.2710(19) Å in **1** (S) to 3.4903(7) Å in **3** (Te). Nevertheless these distances are ~18% shorter than the sum of the respective van der Waals radii and a significant extent of covalent bonding is predicted between Sn and E, similar to the interaction in related phosphorus-tin analogue [Acenap(SnPh₃)(P^{i}Pr₂)],[33] which exhibits a similarly short Sn⋯P distance (~82% $\sum r_{vdW}$) for which a Wiberg Bond Index (WBI) of 0.12 has been computed. As expected, even shorter distances are observed in triorganotin chlorides **5-9** in line with the increased Lewis acidity of the tin centre and much stronger lp(E)−σ*(Sn−Y) donor−acceptor multicentre bonding as a consequence of coordination to a highly electronegative chlorine atom.

This is supported by a noticeable increase in the through-space $J(^{119}Sn,^{77}Se)$ SSCCs observed for **6** (163 Hz) and **8** (142 Hz) compared to triphenyltin analogue **2** (68 Hz). Similar observations are observed in the two geminally bis(*peri*-substituted) systems **10** and **11**, constructed from two distinct acenaphthene fragments which couple through a central tin atom. The coordination of two highly electronegative chlorine atoms in **10** naturally increases the Lewis acidity of the tin centre compared to monosystems **5**, **7** and **9**, leading to marginally shorter distances and stronger lp(S)−σ*(Sn−Cl) donor-acceptor interactions.

EXPERIMENTAL SECTION

All experiments were carried out under an oxygen- and moisture-free nitrogen atmosphere using standard Schlenk techniques and glassware. Reagents were obtained from commercial sources and used as received. Dry solvents were collected from a MBraun solvent system. Elemental analyses were performed at the London Metropolitan University. ¹H and ¹³C NMR spectra were recorded on a Bruker AVANCE 300 MHz spectrometer with δ(H) and δ(C) referenced to external tetramethylsilane. ⁷⁷Se and ¹¹⁹Sn NMR spectra were recorded on a Jeol GSX 270 MHz spectrometer with δ(Se) and δ(Sn) referenced to external dimethylselenide and tetramethylstannane, respectively. Assignments of ¹³C and ¹H NMR spectra were made with the help of H-H COSY and HSQC experiments. All measurements were performed at 25 °C. All values reported for NMR spectroscopy are in parts per million (ppm). Coupling constants (*J*) are given in Hertz (Hz). Mass spectrometry was performed by the University of St Andrews Mass Spectrometry Service. Electrospray Mass Spectrometry (ESMS) was carried out on a Micromass LCT orthogonal accelerator time of flight mass spectrometer. [Acenap(Br)(SPh)] **12**,[27] [Acenap(Br)(SePh)] **13**[27] and [Acenap(Br)(SnPh₃)][32] were prepared following standard literature procedures.

6-(phenylsulfanyl)acenaphth-5-yl-triphenyltin

[Acenap(SnPh₃)(SPh)] (1): To a solution of 5-bromo-6-(phenylsulfanyl)acenaphthene (0.5 g, 1.5 mmol) in dry diethyl ether (30 mL) at −78 °C was added dropwise a 2.5 M solution of *n*-butyllithium in hexane (0.6 mL, 1.5 mmol). The reaction mixture was stirred for 1 h after which a solution of Ph₃SnCl (0.58 g, 1.5 mmol) in diethyl ether (15 mL) was added dropwise to the reaction solution at -78 °C. After stirring at this temperature for 30 min, the reaction mixture was allowed to warm to room temperature and then stirred overnight. The solvent was evaporated *in vacuo* and toluene was added. The mixture was filtered and the toluene was removed *in vacuo*. Colorless crystals were obtained from recrystallisation by diffusion of hexane into a saturated solution of the compound in THF (0.31g, 39%); m.p. 170-172 °C; elemental analysis (Found: C, 70.7; H, 4.5. Calc. for C₃₆H₂₈SnS: C, 70.7; H, 4.6; S, 5.2%); ¹H NMR (270 MHz, CDCl₃, 25 °C, Me₄Si): δ = 7.80 (1 H, d, ³J(¹H,¹H) = 6.7 Hz, ³J(¹H,¹¹⁹Sn) = 66/63 Hz, Acenap 4-H), 7.75 (1 H, d, ³J(¹H,¹H) = 7.2 Hz, Acenap 7-H), 7.60-7.40 (6 H, m, Sn*Ph-o*), 7.37 (1 H, d, ³J(¹H,¹H) = 7.2 Hz, Acenap 8-H), 7.34 (1 H, d, ³J(¹H,¹H) = 6.7 Hz, Acenap 3-H), 7.29-7.18 (9 H, m, Sn*Ph-m,p*), 6.92-6.78 (3 H, m, S*Ph-m,p*), 6.38-6.33 (2 H, m, S*Ph-o*), 3.57-3.45 (4 H, m, Acenap 2x*CH₂*); ¹³C NMR (67.9 MHz, CDCl₃, 25 °C, Me₄Si): δ = 150.0(q), 149.1(q), 142.6(q), 142.5(s, ²J(¹³C,¹¹⁹/¹¹⁷Sn) = 46 Hz), 141.1(q), 139.9(q), 138.8(s), 137.4(s, ²J(¹³C,¹¹⁹/¹¹⁷Sn) = 36 Hz), 130.8(q), 128.7(s), 128.6(s, ²J(¹³C,¹¹⁹/¹¹⁷Sn) = 52 Hz), 128.5(s), 127.0(s), 126.8(q), 125.0(s), 121.0(s), 120.9(s), 30.6(s, Acenap *CH₂*), 30.5(s, Acenap *CH₂*); ¹¹⁹Sn NMR (100.76 MHz, CDCl₃, 25 °C, Me₄Sn): δ = -130.1 (s); MS (ES⁺): *m/z* 634.89 (100%, M+Na).

6-(phenylselanyl)acenaphth-5-yl-triphenyltin

[Acenap(SnPh₃)(SePh)] (2): Synthesis as for compound **1**, but with [Acenap(Br)(SePh)] (0.5 g, 1.3 mmol), 2.5 M *n*-butyllithium (0.5 mL, 1.3 mmol) and Ph₃SnCl (0.50 g, 1.3 mmol). Colorless crystals were obtained from recrystallisation by diffusion of hexane into a saturated solution of the compound in THF (0.42 g, 44%); m.p. 188-190 °C; elemental analysis (Found: C, 65.8; H, 4.2. Calc. for C₃₆H₂₈SnSe: C, 65.7; 4.3 H, %); ¹H NMR (300

MHz, CDCl₃, 25 °C, Me₄Si): δ = 7.88 (1 H, d, $^3J(^1H,^1H)$ = 5.5 Hz, Acenap 4-H), 7.76 (1 H, d, $^3J(^1H,^1H)$ = 6.8 Hz, Acenap-7-H), 7.48-7.27 (6 H, m, Sn*Ph-o*), 7.27-7.05 (11 H, m, Acenap 3,8-H, Sn*Ph-m,p*) 6.87-6.78 (1 H, m, Se*Ph-p*), 6.76-6.68 (2 H, m, Se*Ph-m*), 6.36-6.28 (2 H, m, Se*Ph-o*), 3.45-3.32 (2 H, m, Acenap 2x*CH₂*); ¹³C NMR (75.5 MHz, CDCl₃, 25 °C, Me₄Si): δ = 150.2(q), 149.2(q), 143.3(q), 142.8(s, $^2J(^{13}C,^{119/117}Sn)$ = 45 Hz), 141.2(q), 140.9(s), 140.3(q), 137.3(s, $^2J(^{13}C,^{119/117}Sn)$ = 36 Hz), 136.0(q), 133.2(q), 129.0(s), 128.8(s), 128.6(s), 128.5(s), 125.6(s), 124.9(q), 121.1(s), 120.9(s), 30.7(s, Acenap *CH₂*), 30.5(s, Acenap *CH₂*); ¹¹⁹Sn NMR (100.76 MHz, CDCl₃, Me₄Sn): δ -134.8(s, $^4J(^{119/117}Sn,^{77}Se)$ = 68 Hz); ⁷⁷Se NMR (51.4 MHz, CDCl₃, 25 °C, Me₂Se): δ = 318 (s, $^4J(^{77}Se,^{119/117}Sn)$ = 64 Hz); MS (ES⁺): *m/z* 681.03 (100%, M+Na).

6-(phenyltelluro)acenaphth-5-yl-triphenyltin [Acenap(SnPh₃)(TePh)] (3):

Synthesis as for compound **1**, but with [Acenap(Br)(SnPh₃)] (0.5 g, 1.3 mmol), 2.5 M *n*-butyllithium (0.5 mL, 1.3 mmol) and PhTeTePh (0.53 g, 1.3 mmol). Red crystals were obtained from recrystallisation by diffusion of hexane into a saturated solution of the compound in THF (0.48 g, 79%); m.p. 223-225 °C; elemental analysis (Found: C, 61.0; H, 4.0. Calc. for C₂₆H₃₁SnSeCl: C, 61.2; H, 4.0%); ¹H NMR (300 MHz, CDCl₃, 25 °C, Me₄Si): δ = 8.21 (1 H, d, $^3J(^1H,^1H)$ = 7.1 Hz, Acenap 7-H), 7.70 (1 H, d, $^3J(^1H,^1H)$ = 6.9 Hz, $^3J(^1H,^{119/117}Sn)$ = 66/63 Hz, Acenap 4-H), 7.59-7.24 (9 H, m, Sn*Ph-o,p*), 7.24-7.08 (6 H, m, Sn*Ph-m*), 6.96-6.88 (1 H, m, Te*Ph-p*), 6.82-6.74 (2 H, m, Te*Ph-m*), 6.64-6.58 (2 H, m, Te*Ph-o*), 3.43-3.30 (4 H, m, Acenap 2x*CH₂*); ¹³C NMR (75.5 MHz, CDCl₃, 25 °C, Me₄Si): δ = 147.1(s), 143.4(s), 137.4(s), 137.4(s), 134.1(s), 129.2(s), 129.2(s), 129.1(s), 128.7(s), 128.6(s), 121.7(s), 30.8(s, Acenap *CH₂*), 30.4(s, Acenap *CH₂*); ¹¹⁹Sn NMR (100.76 MHz, CDCl₃, 25 °C, Me₄Sn): δ = -146.8; ¹²⁵Te NMR (85.2 MHz, CDCl₃, 25 °C, Me₂Te): δ = 507; MS (ES⁺): *m/z* 736.83 (100%, M+OMe), 714.81 (100%, M+Li).

6-ethylsulfanylacenaphth-5-yl-triphenyltin [Acenap(SnPh₃)(SEt)] (4):

Synthesis as for compound **1**, but with [Acenap(Br)(SEt)] (0.5 g, 1.7 mmol), 2.5 M *n*-butyllithium (0.7 mL, 1.7 mmol) and Ph₃SnCl (0.66 g, 1.7 mmol). Colorless crystals were obtained from recrystallisation by diffusion of hexane into a saturated solution of the compound in DCM (0.39 g, 41%) m.p. 120-122 °C; elemental analysis (Found: C, 68.2; H, 5.1. Calc. for C₂₂H₃₁ClSSn: C, 68.2; H, 5.0%); ¹H NMR (300 MHz, CDCl₃, 25 °C, Me₄Si): δ = 8.06 (1 H, d, $^3J(^1H,^1H)$ = 6.9 Hz, Acenap 4-H), 7.93 (1 H, d, $^3J(^1H,^1H)$ = 7.2 Hz, Acenap 7-H), 7.90-7.65 (6 H, m, Sn*Ph-o*), 7.60-7.30 (11 H, m, Acenap 3,8-H, Sn*Ph-m,p*), 3.61-3.42 (4 H, m, Acenap 2x*CH₂*), 2.21 (2 H, q, $^3J(^1H,^1H)$ = 7.4 Hz, S*CH₂*CH₃), 0.83 (3 H, t, $^3J(^1H,^1H)$ = 7.4 Hz, SCH₂*CH₃*);¹³C NMR (75.5 MHz, CDCl₃, 25 °C, Me₄Si): δ = 148.8(q), 148.5(q), 143.5(q), 141.8(s), 140.9(q), 139.4(q), 139.1(q), 137.4(s, $^1J(^{13}C,^{119/117}Sn)$ = 35 Hz), 136.7(s), 132.0(q), 131.2(q), 128.8(s), 128.5(s), 120.5(s), 119.9(s), 33.3(s, S*CH₂*CH₃), 30.9(s, Acenap *CH₂*), 30.6(s, Acenap *CH₂*), 14.5(s, SCH₂*CH₃*); ¹¹⁹Sn NMR (100.76 MHz, CDCl₃, 25 °C, Me₄Sn): δ = -135.5(s); MS (ES⁺): *m/z* 586.73 (100%, M+Na).

6-(phenylsulfanyl)acenaphth-5-yl-diphenyltin chloride [Acenap(SnPh₂Cl)[SPh]] (5):

Synthesis as for compound **1**, but with [Acenap(Br)(SPh)] (0.5 g, 1.5 mmol), 2.5 M *n*-butyllithium (0.6 mL, 1.5 mmol) and Ph₂SnCl₂ (0.52 g, 1.5 mmol). Colorless crystals were obtained from recrystallisation by diffusion of hexane into a saturated solution of the compound in THF (0.33 g, 40%); m.p. 75-77 °C; elemental analysis (Found: C, 63.0; H, 4.0. Calc. for C₃₀H₂₃SnSCl: C, 63.2; H, 4.1%); ¹H NMR (300 MHz, CDCl₃, 25 °C, Me₄Si): δ = 8.84 (1 H, d, $^3J(^1H,^1H)$ = 7.0 Hz, $^3J(^1H,^{119/117}Sn)$ = 77/74 Hz, Acenap 4-H), 7.91 (1 H, d, $^3J(^1H,^1H)$ = 8.3 Hz, Acenap 7-H), 7.66 (1 H, d, $^3J(^1H,^1H)$ = 7.0 Hz, Acenap 3-H), 7.61-7.53 (6 H, m, Sn*Ph-o*), 7.52-7.47 (1 H, m, Acenap 8-

H), 7.29-7.09 (9 H, m, Sn*Ph-m,p*), 6.97-6.91 (1 H, m, S*Ph-p*), 6.88-6.80 (2 H, m, S*Ph-m*), 6.49-6.43 (2 H, m, S*Ph-o*), 3.61-3.49 (4 H, m, Acenap 2x*CH₂*); ¹³C NMR (75.5 MHz, CDCl₃, 25 °C, Me₄Si): δ = 150.7(q), 149.7(q), 141.3(s, $^2J(^{13}C,^{119/117}Sn)$ = 39 Hz), 141.2(q), 140.7(q), 139.1(q), 136.3(q), 135.8(s, $^2J(^{13}C,^{119/117}Sn)$ = 47 Hz), 132.8(q), 129.1(s), 128.7(s), 128.5(s), 127.6(s), 127.2(s), 126.1(s), 123.5(q), 121.5(s), 121.1(s), 30.2(s, Acenap *CH₂*), 30.4(s, Acenap *CH₂*);¹¹⁹Sn NMR (100.76 MHz, CDCl₃, 25 °C, Me₄Sn): δ = -116.9; MS (ES⁺): *m/z* 535.06 (100%, M-Cl).

6-(phenylselanyl)acenaphth-5-yl-diphenyltin chloride [Acenap(SnPh₂Cl)[SePh]] (6):

Synthesis as for compound **1**, but with [Acenap(Br)(SePh)] (0.5 g, 1.3 mmol), 2.5 M *n*-butyllithium (0.5 mL, 1.3 mmol) and Ph₂SnCl₂ (0.45 g, 1.3 mmol). Colorless crystals were obtained from recrystallisation by diffusion of hexane into a saturated solution of the compound in THF (0.31 g, 39%); m.p. 152-154 °C; elemental analysis (Found: C, 58.4; H, 3.9. Calc. for C₂₆H₃₁SnSeCl: C, 58.4; H, 3.8%);¹H NMR (300 MHz, CDCl₃, 25 °C, Me₄Si): δ = 8.75 (1 H, d, $^3J(^1H,^1H)$ = 7.1 Hz, $^3J(^1H,^{119/117}Sn)$ = 78/75 Hz, Acenap 4-H), 7.72 (1 H, d, $^3J(^1H,^1H)$ = 7.1 Hz, Acenap 7-H), 7.51 (1 H, d, $^3J(^1H,^1H)$ = 7.1 Hz, Acenap 3-H), 7.49-7.42 (6 H, m, Sn*Ph-o*), 7.29-6.99 (10 H, m, Acenap 8-H, Sn*Ph-m,p*), 6.89-6.78 (1 H, m, Se*Ph-p*), 6.74-6.63 (2 H, m, Se*Ph-m*), 6.35-6.24 (2 H, m, Se*Ph-o*), 3.48-3.34 (4 H, m, Acenap 2x*CH₂*); ¹³C NMR (75.5 MHz, CDCl₃, 25 °C, Me₄Si): δ = 151.3(q), 150.1(q), 146.9(q), 142.8(q), 142.2(s), 141.3(q), 137.3(s), 136.1(s), 133.2(q), 132.0(q), 130.9(s), 129.6(s), 129.0(s), 128.8(s), 126.8(s), 122.5(q), 121.9(s), 120.4(s), 30.8(s, Acenap *CH₂*), 30.6(s, Acenap *CH₂*);¹¹⁹Sn NMR (100.76 MHz, CDCl₃, 25 °C, Me₄Sn): δ = -131.3(s, $^4J(^{119/117}Sn,^{77}Se)$ = 163 Hz); ⁷⁷Se NMR (51.4 MHz, CDCl₃, 25 °C, Me₂Se): δ = 266 (s, $^4J(^{77}Se,^{119/117}Sn)$ = 160 Hz); MS (ES⁺): *m/z* 580.81 (100%, M-Cl).

6-(phenylsulfanyl)acenaphth-5-yl-dibutyltin chloride [Acenap(SnBu₂Cl)(SPh)] (7):

Synthesis as for compound **1**, but with [Acenap(Br)(SPh)] (0.5 g, 1.5 mmol), 2.5 M *n*-butyllithium (0.6 mL, 1.5 mmol) and Bu₂SnCl₂ (0.46 g, 1.5 mmol). Colorless crystals were obtained from recrystallisation by diffusion of hexane into a saturated solution of the compound in THF (0.18 g, 23%); m.p. 82-84 °C; elemental analysis (Found: C, 58.8; H, 5.8. Calc. for C₂₆H₃₁SnSCl: C, 58.9; H, 5.9%); ¹H NMR (300 MHz, CDCl₃, 25 °C, Me₄Si): δ = 8.44 (1 H, d, $^3J(^1H,^1H)$ = 7.0 Hz, $^3J(^1H,^{119/117}Sn)$ = 64/61 Hz, Acenap 4-H), 7.70 (1 H, d, $^3J(^1H,^1H)$ = 6.4 Hz, Acenap 7-H), 7.44 (1 H, d, $^3J(^1H,^1H)$ = 7.8 Hz, Acenap 3-H), 7.27 (1 H, d, $^3J(^1H,^1H)$ = 7.1 Hz, Acenap 8-H), 7.12-7.02 (3 H, m, S*Ph-m,p*), 6.84-6.81 (2 H, m, S*Ph-o*), 3.40-3.30 (4 H, m, Acenap 2x*CH₂*), 1.50-1.25 (8 H, m, 2x*CH₂-α*,2x*CH₂-β*), 1.04 (4 H, h, $^3J(^1H,^1H)$ = 7.3 Hz, 2x*CH₂-γ*), 0.65 (6 H, t, $^3J(^1H,^1H)$ = 7.2 Hz, 2x*CH₃-δ*); ¹³C NMR (75.5 MHz, CDCl₃, 25 °C, Me₄Si): δ = 151.1(q), 148.8(q), 140.9(s), 139.7(q), 137.8(s), 137.3(q), 132.9(q), 129.7(s), 129.5(s), 127.3(s), 126.3(q), 123.6(q), 121.7(s), 120.7(s), 30.8(s, Acenap *CH₂*), 30.6(s, Acenap *CH₂*), 28.7(s, 2x*CH₂-β*), 26.9(s, 2x*CH₂-γ*), 22.1(s, 2x*CH₂-α*), 13.9(s, 2x*CH₃-δ*); ¹¹⁹Sn NMR (100.76 MHz, CDCl₃, 25 °C, Me₄Sn): δ = 3.56; MS (ES⁺): *m/z* 435.09 (100%, M-BuCl).

6-(phenylselanyl)acenaphth-5-yl-dibutyltin chloride [Acenap(SnBu₂Cl)(SePh)] (8):

Synthesis as for compound **1**, but with [Acenap(Br)(SePh)] (0.5 g, 1.3 mmol), 2.5 M *n*-butyllithium (0.5 mL, 1.3 mmol) and Bu₂SnCl₂ (0.39 g, 1.3 mmol). Yellow crystals were obtained from recrystallisation by diffusion of hexane into a saturated solution of the compound in THF (0.46 g, 62%); m.p. 108-110 °C; elemental analysis (Found: C, 54.3; H, 5.3. Calc for C₂₆H₃₁SnSeCl: C, 54.2; H, 5.4%); ¹H NMR (300 MHz, CDCl₃, 25 °C, Me₄Si): δ = 8.50 (1 H, d, $^3J(^1H,^1H)$ = 7.1 Hz, $^3J(^1H,^{119/117}Sn)$ = 64/61 Hz, Acenap 4-H), 7.83 (1 H, d, $^3J(^1H,^1H)$ = 7.1 Hz, Acenap 7-H), 7.43 (1 H, d, $^3J(^1H,^1H)$ = 7.0 Hz, Acenap 3-H), 7.25 (1 H, d, $^3J(^1H,^1H)$ = 7.2 Hz, Acenap 8-H), 7.12-7.03 (3

H, m, SePh-*m,p*), 6.88-6.81 (2 H, m, SePh-*o*), 3.45-3.33 (4 H, m, Acenap 2xCH_2), 1.50-1.25 (8 H, m, 2xCH_2-α,2xCH_2-β), 1.05 (4 H, h, $^3J(^1H,^1H)$ = 7.4 Hz, 2xCH_2-γ), 0.65 (6 H, t, $^3J(^1H,^1H)$ = 7.2 Hz, 2xCH_3-δ); ^{13}C NMR (75.5 MHz, CDCl$_3$, 25 °C, Me$_4$Si): δ = 151.3(q), 148.9(q), 141.4(s), 141.2(q), 140.2(q), 139.6(s), 135.3(q), 133.1(q), 130.0(s), 128.8(s), 127.5(s), 122.1(q), 121.6(s), 120.8(s), 30.7(s, Acenap CH_2), 30.6(s, Acenap CH_2), 28.9(s, 2xCH_2-β), 26.9(s, 2xCH_2-γ), 23.2(s, 2xCH_2-α), 13.9(s, 2xCH_3-δ); ^{119}Sn NMR (100.76 MHz, CDCl$_3$, 25 °C, Me$_4$Sn): δ = -12.4; ^{77}Se NMR (51.4 MHz, CDCl$_3$, 25 °C, Me$_2$Se): δ = 271 (s, $^4J(^{77}Se,^{119/117}Sn)$ = 138 Hz) MS (ES$^+$): *m/z* 556.65 (100%, M-Cl+OH), 540.71 (40%, M-Cl).

6-ethylsulfanylacenapth-5-yl-dibutyltin chloride [Acenap(SnBu$_2$Cl)(SEt)] (9): Synthesis as for compound **1**, but with [Acenap(Br)(SEt)] (0.5 g, 1.7 mmol), 2.5 M *n*-butyllithium (0.7 mL, 1.7 mmol) and Bu$_2$SnCl$_2$ (0.52 g, 1.7 mmol). Colorless crystals were obtained after recrystallisation from THF at -30 °C (0.43 g, 53%); m.p. 54-56 °C; elemental analysis (Found: C, 55.0; H, 6.4. Calc. for C$_{22}$H$_{31}$ClSSn: C, 54.9; H, 6.5%); ^{1}H NMR (300 MHz, CDCl$_3$, 25 °C, Me$_4$Si): δ = 8.43 (1 H, d, $^3J(^1H,^1H)$ = 7.1 Hz, $^3J(^1H,^{119/117}Sn)$ = 66/63 Hz, Acenap 4-H), 7.66 (1 H, d, $^3J(^1H,^1H)$ = 7.1 Hz, Acenap 7-H), 7.38 (1 H, d, $^3J(^1H,^1H)$ = 6.8 Hz, Acenap 3-H), 7.22 (1 H, d, $^3J(^1H,^1H)$ = 7.5 Hz, Acenap 8-H), 3.42-3.29 (4 H, m, Acenap 2xCH_2), 2.68 (2 H, q, $^3J(^1H,^1H)$ = 6.8 Hz, SCH_2CH$_3$), 1.17 (3 H, t, $^3J(^1H,^1H)$ = 7.7 Hz, SCH$_2$CH_3), 1.77-1.53 (8 H, m, 2xCH_2-α,2xCH_2-β), 1.25 (4 H, h, $^3J(^1H,^1H)$ = 7.0 Hz, 2xCH_2-γ), 0.77 (6 H, t, $^3J(^1H,^1H)$ = 7.7 Hz, 2xCH_3-δ); ^{13}C NMR (75.5 MHz, CDCl$_3$, 25 °C, Me$_4$Si): δ = 150.0(q), 148.7(q), 140.8(q), 140.4(s), 138.8(q), 136.6(s), 133.6(q), 125.5(q), 121.4(s), 119.7(s), 33.7(s, SCH_2CH$_3$), 30.7(s, Acenap CH_2), 30.6(s, Acenap CH_2), 28.9(s, $^1J(^{13}C,^{119/117}Sn)$ = 31.0, 2xCH_2-β,), 27.1(s, 2xCH_2-α),22.3(s, 2xCH_2-γ), 14.3(s, SCH$_2$CH_3), 14.0(s, 2xCH_3-δ); ^{119}Sn NMR (100.76 MHz, CDCl$_3$, 25 °C, Me$_4$Sn): δ = -12.3.(s).

Bis(6-(phenylsulfanyl)acenaphthen-5-yl)dichlorostannane [{Acenap(SPh)}$_2$SnCl$_2$] (10): Synthesis as for compound **1**, but with [Acenap(Br)(SPh)] (0.5 g, 1.5 mmol), 2.5 M *n*-butyllithium (0.6 mL, 1.5 mmol) and SnCl$_4$ (0.39 g, 1.5 mmol) in hexane (15 mL). Colorless crystals were obtained from recrystallisation by diffusion of hexane into a saturated solution of the compound in THF (0.1 g, 19%); m.p. 224-226 °C; Elemental analysis (Found: C, 54.7; H, 4.2. Calc. for C$_{28}$H$_{26}$SnS$_2$Cl$_2$: C, 54.6; H, 4.3%); ^{1}H NMR (300 MHz, CDCl$_3$, 25 °C, Me$_4$Si): δ = 8.54 (2 H, d, $^3J(^1H,^1H)$ = 7.1 Hz, $^3J(^1H,^{119/117}Sn)$ = 120/114 Hz, Acenap 2x4-H), 7.53 (2 H, d, $^3J(^1H,^1H)$ = 7.1 Hz, $^4J(^1H,^{119/117}Sn)$ = 26 Hz, Acenap 2x3-H), 7.45 (2 H, d, $^3J(^1H,^1H)$ = 7.1 Hz, Acenap 2x7-H), 7.21 (2 H, d, $^3J(^1H,^1H)$ = 7.1 Hz, Acenap 2x8-H), 6.77-6.66 (6 H, m, SPh-*m,p*), 6.23-6.20 (4 H, m, SPh-*o*), 3.52-3.37 (8 H, m, Acenap 4xCH_2); ^{13}C NMR (75.5 MHz, CDCl$_3$, 25 °C, Me$_4$Si): δ = 150.5(q), 149.6(q), 140.8(q), 137.9(s), 137.2(s), 137.1(q), 136.1(q), 135.7(q), 128.6(s), 126.6(s), 126.3(q), 122.1(s), 121.7(s), 120.8(s), 30.9(s, Acenap 2xCH_2), 26.0(s, Acenap 2xCH_2); ^{119}Sn NMR (100.76 MHz, CDCl$_3$, 25 °C, Me$_4$Sn): δ = -192.0(s).

Bis(6-(phenylsulfanyl)acenaphthen-5-yl)diphenylstannane [{Acenap(SPh)}$_2$SnPh$_2$] (11): Synthesis as for compound **1**, but with [Acenap(Br)(SPh)] (0.5 g, 1.5 mmol), 2.5 M *n*-butyllithium (0.6 mL, 1.5 mmol) and Ph$_2$SnCl$_2$ (0.52 g, 1.5 mmol). Colorless crystals were obtained from recrystallisation by diffusion of hexane into a saturated solution of the compound in THF (0.26 g, 44%); m.p. 220-222 °C; elemental analysis (Found: C, 72.4; H, 4.6. Calc. for C$_{48}$H$_{36}$SnS$_2$: C, 72.5; H, 4.6%;); ^{1}H NMR (300 MHz, CDCl$_3$, 25 °C, Me$_4$Si): δ = 8.71 (2 H, d, $^3J(^1H,^1H)$ = 7.1 Hz, $^3J(^1H,^{119/117}Sn)$ = 63/60 Hz, Acenap 2x4-H), 7.66 (2 H, d, $^3J(^1H,^1H)$ = 7.2 Hz, Acenap 2x7-H), 7.55 (2 H, d, $^3J(^1H,^1H)$ = 7.0 Hz, Acenap 2x3-H), 7.49-7.42 (4 H, m, SnPh-*o*), 7.30-7.23 (2 H,

m, Acenap 2x8-H), 7.17-7.07 (6 H, m, SPh-*m,p*), 6.87-6.77 (2 H, m, SPh-*p*), 6.77-6.68 (4 H, m, SPh-*m*), 6.40-6.31 (4 H, m, SPh-*o*), 3.53-3.38 (8 H, m, Acenap 4xCH_2); ^{13}C NMR (75.5 MHz, CDCl$_3$, 25 °C, Me$_4$Si): δ = 151.0(q), 149.9(q), 142.0(q), 141.6(s), 140.1(q), 138.0(s), 136.7(q), 136.2(s), 131.5(s), 129.1(s), 128.9(s), 128.7(s), 127.6(s), 126.5(s), 125.3(q), 121.9(s), 121.0(s), 30.9(s, Acenap 2xCH_2), 30.8(s, Acenap 2xCH_2); ^{119}Sn NMR (100.76 MHz, CDCl$_3$, 25 °C, Me$_4$Sn): δ = -166.9(s); MS (ES$^+$): *m/z* 535.05 (100%, M-Acenap(SPh)).

5-bromo-6-ethylsulfanylacenaphthene [Acenap(Br)(SEt)] (15): To a solution of 5,6-dibromoacenaphthene (10.0 g, 32.0 mmol) in dry diethyl ether (60 mL) at −78 °C was added dropwise a 2.5 M solution of *n*-butyllithium in hexane (12.1 mL, 32.2 mmol). The reaction mixture was stirred for 1 h after which a solution of diethyl disulfide (4 mL, 32.2 mmol) in diethyl ether (10 mL) was added dropwise to the reaction solution at -78 °C. After stirring at this temperature for 30 min, the reaction mixture was allowed to warm to room temperature and then washed with a 0.1 N NaOH solution (2 x 50 mL). The organic layer was the collected, dried over MgSO$_4$ and concentrated under reduced pressure to afford the title compound as a yellow powder. Colorless crystals were obtained from recrystallisation by diffusion of hexane into a saturated solution of the compound in DCM (2.99 g, 34%); m.p. 79-81 °C; elemental analysis (Found: C, 57.4; H, 4.3. Calc. for C$_{14}$H$_{13}$SBr: C, 57.3; H, 4.5%); ^{1}H NMR (300 MHz, CDCl$_3$, 25 °C, Me$_4$Si): δ = 7.70 (1 H, d, $^3J(^1H,^1H)$ = 7.4 Hz, Acenap 4-H), 7.49 (1 H, d, $^3J(^1H,^1H)$ = 7.4 Hz, Acenap 7-H), 7.18 (1 H, d, $^3J(^1H,^1H)$ = 7.4 Hz, Acenap 8-H), 7.05 (1 H, d, $^3J(^1H,^1H)$ = 7.4 Hz, Acenap 3-H), 3.29 (4 H, s, Acenap 2xCH_2), 2.96 (2 H, q, $^3J(^1H,^1H)$ = 7.5 Hz, SCH_2CH$_3$,), 1.33 (3 H, t, $^3J(^1H,^1H)$ = 7.5 Hz, SCH$_2$CH_3,);^{13}C NMR (75.5 MHz, CDCl$_3$, 25 °C, Me$_4$Si): δ = 146.9(q), 145.7(q), 141.9(q), 135.9(q), 135.0(s), 132.0(s), 129.6(q), 120.7(s), 120.2(s), 114.5(q), 30.4(s, SCH$_2$CH$_3$), 30.1(s, Acenap CH_2), 30.0(s, Acenap CH_2), 13.6(s, SCH$_2$CH$_3$); MS (ES$^+$): *m/z* 293.99 (100%, M+).

Crystal structure analyses. X-ray crystal structures for **1**, **2**, **6-8**, **10** and **11** were determined at −148(1) °C using a Rigaku MM007 high-brilliance RA generator (Mo Kα radiation, confocal optic) and Saturn CCD system. At least a full hemisphere of data was collected using ω scans. Intensities were corrected for Lorentz, polarization, and absorption. Data for compounds **3-5** and **14** were collected at −148(1) °C with a Rigaku SCXmini CCD area detector with graphite-monochromated Mo-*K*α radiation (*λ*= 0.71073 Å). Data were corrected for Lorentz, polarisation and absorption. Data for compound **9** were collected at −148(1) °C using a Rigaku MM007 high-brilliance RA generator (Mo Kα radiation, confocal optic) and Mercury CCD system. At least a full hemisphere of data was collected using ω scans. Data for all compounds analyzed were collected and processed using CrystalClear (Rigaku).[41] Structures were solved by direct methods[42] and expanded using Fourier techniques.[43] Non-hydrogen atoms were refined anisotropically. Hydrogen atoms were refined using the riding model. All calculations were performed using the CrystalStructure[44] crystallographic software package except for refinement, which was performed using SHELXL2013.[45] These X-ray data can be obtained free of charge via www.ccdc.cam.ac.uk/conts/retrieving.html or from the Cambridge Crystallographic Data Centre, 12 Union Road, Cambridge CB2 1EZ, UK; fax (+44) 1223-336-033; e-mail: deposit@ccdc.cam.ac.uk; CCDC nos. 1020875-1020898.

ASSOCIATED CONTENT

Supporting Information

X-ray crystallographic data and figures. This material is available free of charge via the Internet at http://pubs.acs.org.

AUTHOR INFORMATION

Corresponding Author

*J.D.W.: fax, (+44) 1334 463384; e-mail, jdw3@st-andrews.ac.uk.

Notes

The authors declare no competing financial interests.

REFERENCES

(1) (a) Coulson, C. A.; Daudel, R.; Robertson, J. M. *Proc., R. Soc. London, Ser. A* **1951**, *207*, 306. (b) Cruickshank, D. W. *Acta Crystallogr.* **1957**, *10*, 504. (c) Brock, C. P.; Dunitz, J. D. *Acta Crystallogr., Sect. B* **1982**, *38*, 2218. (d) Oddershede, J.; Larsen, S. *J. Phys. Chem. A* **2004**, *108*, 1057.

(2) Hazell, A. C.; Hazell, R. G.; Nørskov-Lauritsen, L.; Briant, C. E.; Jones, D. W. *Acta Crystallogr., Sect. C* **1986**, *42*, 690.

(3) For example, see: (a) Katz, H. E. *J. Am. Chem. Soc.* **1985**, *107*, 1420. (b) Alder, R. W.; Bowman, P. S.; Steel, W. R. S.; Winterman, D. R. *Chem. Commun.* **1968**, 723. (c) Costa, T.; Schimdbaur, H. *Chem. Ber.* **1982**, *115*, 1374. (d) Karaçar, A.; Freytag, M.; Thönnessen, H.; Omelanczuk, J.; Jones, P. G.; Bartsch, R.; Schmutzler, R. *Heteroat. Chem.* **2001**, *12*, 102. (e) Glass, R. S.; Andruski, S. W.; Broeker, J. L.; Firouzabadi, H.; Steffen, L. K.; Wilson, G. S. *J. Am. Chem. Soc.* **1989**, *111*, 4036. (f) Fuji, T.; Kimura, T.; Furukawa, N. *Tetrahedron Lett.* **1995**, *36*, 1075. (g) Schiemenz, G. P. *Z. Anorg. All. Chem.* **2002**, *628*, 2597. (h) Corriu, R. J. P.; Young, J. C. *Hypervalent Silicon Compounds. In Organic Silicon Compounds*; Patai, S., Rappoport, Z., Eds.; Wiley: Chichester, U.K., **1989**; Vols. 1 and 2.

(4) Balasubramaniyan, V. *Chem. Rev.* **1966**, *66*, 567.

(5) Kilian, P.; Knight, F. R.; Woollins, J. D. *Chem. Eur. J.* **2011**, *17*, 2302.

(6) (a) Schmidbaur, H.; Öller, H.-J.; Wilkinson, D. L.; Huber, B.; Müller, G. *Chem. Ber.* **1989**, *122*, 31. (b) Fujihara, H.; Furukawa, N. *J. Mol. Struct.* **1989**, *186*, 261. (c) Fujihara, H.; Akaishi, R.; Erata, T.; Furukawa, N. *J. Chem. Soc., Chem. Commun.* **1989**, 1789. (d) Handal, J.; White, J. G.; Franck, R. W.; Yuh, Y. H.; Allinger, N. L. *J. Am. Chem. Soc.* **1977**, *99*, 3345. (e) Blount, J. F.; Cozzi, F.; Damewood, J. R.; Iroff, D. L.; Sjöstrand, U.; Mislow, K. *J. Am. Chem. Soc.* **1980**, *102*, 99. (f) Anet, F. A. L.; Donovan, D.; Sjöstrand, U.; Cozzi, F.; Mislow, K. *J. Am. Chem. Soc.* **1980**, *102*, 1748. (g) Hounshell, W. D.; Anet, F. A. L.; Cozzi, F.; Damewood, J. R., Jr.; Johnson, C. A.; Sjöstrand, U.; Mislow, K. *J. Am. Chem. Soc.* **1980**, *102*, 5941. (h) Schrock, R.; Angermaier, K.; Sladek, A.; Schmidbaur, H. *Organometallics* **1994**, *13*, 3399.

(7) (a) Nakanishi, W.; Hayashi, S.; Toyota, S. *Chem. Commun.* **1996**, 371. (b) Nakanishi, W.; Hayashi, S.; Sakaue, A.; Ono, G.; Kawada, Y. *J. Am. Chem. Soc.* **1998**, *120*, 3635. (c) Nakanishi, W.; Hayashi, S.; Toyota, S. *J. Org. Chem.* **1998**, *63*, 8790. (d) Hayashi, S.; Nakanishi, W. *J. Org. Chem.* **1999**, *64*, 6688. (e) Nakanishi, W.; Hayashi, S.; Uehara, T. *J. Phys. Chem. A* **1999**, *103*, 9906. (f) Nakanishi, W.; Hayashi, S.; Uehara, T. *Eur. J. Org. Chem.* **2001**, 3933. (g) Nakanishi, W.; Hayashi, S. *Phosphorus Sulfur Silicon Relat. Elem.* **2002**, *177*, 1833. (h) Nakanishi, W.; Hayashi, S.; Arai, T. *Chem. Commun.* **2002**, 2416. (i) Hayashi, S.; Nakanishi, W. *J. Org. Chem.* **2002**, *67*, 38. (j) Nakanishi, W.; Hayashi, S.; Itoh, N. *Chem. Commun.* **2003**, 124. (k) Hayashi, S.; Wada, H.; Ueno, T.; Nakanishi, W. *J. Org. Chem.* **2006**, *71*, 5574. (l) Hayashi, S.; Nakanishi, W. *Bull. Chem. Soc. Jpn.* **2008**, *81*, 1605. (m) Hayashi, S.; Yamane, K.; Nakanishi, W. *Bioinorg. Chem. App.* **2009**, *2009*, 347359, **doi:10.1155/2009/347359**. (n) Nakai, T.; Nishino, M.; Hayashi, S.; Hashimoto, M.; Nakanishi, W. *Dalton Trans.* **2012**, *41*, 7485.

(8) Ray, M. J.; Randall, R. A. M.; Athukorala Arachchige, K. S; Slawin, A. M. Z.; Bühl, M.; Lebl, T; Kilian, P *Inorg. Chem.* **2013**, *52*, 4346.

(9) Chalmers, A. B.; Athukorala Arachchige, K. S; Prentis, J. K. D.; Knight, F. R.; Kilian, P.; Slawin, A. M. Z.; Woollins, J. D. *Inorg. Chem.* **2014**, *53*, 8795.

(10) Somisara, D. M. U. K.; Bühl, M.; Lebl, T; Richardson, N. V.; Slawin, A. M. Z.; Woollins, J. D.; Kilian, P. *Chem. Eur. J.* **2011**, *17*, 2666.

(11) Omelańczuk, J.; Karaçar, A.; Freytag, M.; Jones, P. G.; Bartsch, R.; Mikołajczyk, M.; Schmutzler, R. *Inorg. Chim. Acta* **2003**, *350*, 583.

(12) Allen, F. H. *Acta Cryst.* **2002**, *B58*, 380 "The Cambridge Structural Database: a quarter of a million crystal structures and rising" **DOI: 10.1107/S0108768102003890**.

(13) Beckmann, J.; Hupf, E.; Lork, E. *Main Group Met. Chem.* **2013**; *36*, 145.

(14) (a) Blount, J. F.; Cozzi, F.; Damewood, Jr. J. R.; Iroff, L. D.; Sjöstrand, U.; Mislow, K. *J. Am. Chem. Soc.* **1980**, *102*, 99. (b) Seyferth, D.; Vick, S. C. *J. Organomet. Chem.* **1977**, *141*, 173.

(15) (a) Wawrzyniak, P.; Slawin, A. M. Z.; Woollins, J. D.; Kilian, P. *Dalton Trans.* **2010**, *39*, 85. (b) Wawrzyniak, P.; Fuller, A. L.; Slawin, A. M. Z.; Kilian, P. *Inorg. Chem.* **2009**, *48*, 2500. (c) Surgenor, B. A.; Bühl, M.; Slawin, A. M. Z.; Woollins, J. D.; Kilian, P. *Angew. Chem., Int. Ed.* **2012**, *51*, 10150.

(16) Knight, F. R.; Randall, R. A. M.; Roemmele, T. L.; Boeré, R. T.; Bode, B. E.; Crawford, L.; Bühl, M.; Slawin, A. M. Z.; Woollins, J. D. *ChemPhysChem*, **2013**, *14*, 3199.

(17) Aucott, S. M.; Milton, H. L.; Robertson, S. D.; Slawin, A. M. Z.; Woollins, J. D. *Heteroat. Chem.* **2004**, *15*, 530.

(18) (a) Meinwald, J.; Dauplaise, D.; Wudl, F.; Hauser, J. J. *J. Am. Chem. Soc.* **1977**, *99*, 255. (b) Ashe, A. J., III; Kampf, J. W.; Savla, P. M. *Heteroat. Chem.* **1994**, *5*, 113. (c) Lanfrey, M. C. R. *Acad. Sci.* **1911**, *152*, 92. (d) Price, W. B.; Smiles, S. *J. Chem. Soc.* **1928**, 2372. (e) Zweig, A.; Hoffman, A. K. *J. Org. Chem.* **1965**, *30*, 3997. (f) Kilian, P.; Slawin, A. M. Z.; Woollins, J. D. *Dalton Trans.* **2006**, 2175. (g) Kilian, P.; Philp, D.; Slawin, A. M. Z.; Woollins, J. D. *Eur. J. Inorg. Chem.* **2003**, 249.

(19) (a) Chuit, C.; Reyé, C. *Eur. J. Inorg. Chem.* **1998**, 1847. (b) Bushuk, S. B.; Carré, F. H.; Guy, D. M. H.; Douglas, W. E.; Kalvinkovskaya, Y. A.; Klapshina, L. G.; Rubinov, A. N.; Stupak, A. P.; Bushuk, B. A. *Polyhedron* **2004**, *23*, 2615. (c) Chauhan, M.; Chuit, C.; Fruchier, A.; Reyé, C. *Inorg. Chem.* **1999**, *38*, 1336. (d) Carré, F. H.; Chauhan, M.; Chuit, C.; Corriu, R. J. P.; Reyé, C. *Phosphorus Sulfur Silicon Relat. Elem.* **1997**, *123*, 181.

(20) (a) Schiemenz, G. P. *Z. Anorg. Allg. Chem.* **2002**, *628*, 2597. (b) Schiemenz, G. P. *Z. Naturforsch., B* **2006**, *61*, 535. (c) Schiemenz, G. P.; Nather, C.; Porksen, S. *Z. Naturforsch., B* **2003**, *58*, 59. (d) Schiemenz, G. P.; Nather, C.; Porksen, S. *Z. Naturforsch., B* **2003**, *58*, 663. (e) Schiemenz, G. P.; Nather, C.; Porksen, S. *Z. Naturforsch. B* **2003**, *58*, 715. (f) Schiemenz, G. P. *Phosphorus Sulfur Silicon Relat. Elem.* **2009**, *184*, 2247. (g) Schiemenz, G. P. *Phosphorus Sulfur Silicon Relat. Elem.* **2000**, *163*, 185. (h) Schiemenz, G. P.; Bukowski, R.; Eckholtz, L.; Varnskühler, B. *Z. Naturforsch., B* **2000**, *55*, 12. (i) Schiemenz, G. P.; Porksen, S.; Dominiak, P. M.; Wozniak, K. *Z. Naturforsch., B* **2002**, *57*, 8. (j) Dominiak, P. M.; Petersen, S.; Schiemenz, B.; Schiemenz, G. P.; Wozniak, K. *J. Mol. Struct. (THEOCHEM)* **2005**, *751*, 172.

(21) Schiemenz, G. P.; Porksen, S.; Nather, C. *Z. Naturforsch., B* **2000**, *55*, 841. (22) Carré, F. H.; Chuit, C.; Corriu, R. J. P.; Douglas, W. E.; Guy, D. M. H.; Reyé, C. *Eur. J. Inorg. Chem.* **2000**, 647.

(23) (a) Chandrasekaran, A.; Timosheva, N. V.; Day, R. O.; Holmes, R. R. *Inorg. Chem.* **2000**, *39*, 1338. (b) Hellwinkel, D.; Lindner, W.; Wilfinger, H.-J. *Tetrahedron Lett.* **1969**, *10*, 3423. (c) Hellwinkel, D.; Lindner, W.; Wilfinger, H.-J. *Chem. Ber.* **1974**, *107*, 1428. (d) Day, R. O.; Holmes, R. R. *Inorg. Chem.* **1980**, *19*, 3609.

(24) Panda, A.; Mugesh, G.; Singh, H. B.; Butcher, R. J. *Organometallics* **1999**, *18*, 1986.

(25) (a) Beckmann, J.; Bolsinger, J.; Duthie, A.; Finke, P. *Dalton. Trans.* **2013**, *42*, 12193. (b) Beckmann, J.; Bolsinger, J.; Duthie, A. *Chem. Eur. J.* **2011**, *17*, 930.

(26) (a) Knight, F. R.; Fuller, A. L.; Bühl, M.; Slawin, A. M. Z.; Woollins, J. D. *Chem. Eur. J.* **2010**, *16*, 7503. (b) Knight, F. R.; Fuller, A. L.; Bühl, M.; Slawin, A. M. Z.; Woollins, J. D. *Chem. Eur. J.* **2010**, *16*, 7605. (c) Knight, F. R.; Fuller, A. L.; Bühl, M.; Slawin, A. M. Z.; Woollins, J. D. *Chem. Eur. J.* **2010**, *16*, 7617. (d) Knight, F. R.; Randall, R. A. M.; Athukorala Arachchige, K. S.; Wakefield, L.; Griffin, J. M.; Ashbrook, S. E.; Bühl, M.; Slawin, A. M. Z.; Woollins, J. D. *Inorg. Chem.* **2012**, *51*, 11087. (e) Diamond, L. M.; Knight, F. R.; Athukorala Arachchige, K. S.;

Randall, R. A. M.; Bühl, M.; Slawin, A. M. Z.; Woollins, J. D. *Eur. J. Inorg. Chem*. **2014**, 1512. (f) Stanford, M. W.; Knight, F. R.; Athukorala Arachchige, K. S.; Sanz Camacho, P.; Ashbrook, S. E.; Bühl, M.; Slawin, A. M. Z.; Woollins, J. D. *Dalton Trans*. **2014**, *43*, 6548.

(27) Aschenbach, L. K.; Knight, F. R.; Randall, R. A. M.; Cordes, D. B.; Baggott, A.; Bühl, M.; Slawin, A. M. Z.; Woollins, J. D. *Dalton Trans*. **2012**, *41*, 3141.

(28) (a) Knight, F. R.; Fuller, A. L.; Bühl, M.; Slawin, A. M. Z.; Woollins, J. D. *Inorg. Chem.* **2010**, *49*, 7577. (b) Knight, F. R.; Athukorala Arachchige, K. S.; Randall, R. A. M.; Bühl, M.; Slawin, A. M. Z.; Woollins, J. D. *Dalton Trans*. **2012**, *41*, 3154.

(29) Bühl, M.; Knight, F. R.; Křístková, A.; Malkin Ondík, I.; Malkina, O. L.; Randall, R. A. M.; Slawin, A. M. Z.; Woollins, J. D. *Angew. Chem.* **2013**, *125*, 2555; *Angew. Chem., Int. Ed*. **2013**, *52*, 2495.

(30) Wiberg, K. B. *Tetrahedron* **1968**, *24*, 1083.

(31) Jastrzebski, J. T. B. H.; Boersma, J.; Esch, P. M.; van Koten, G. *Organometallics* **1991**, *10*, 930.

(32) Athukorala Arachchige, K. S.; Sanz Camacho, P.; Ray, M. J.; Chalmers, B. A.; Knight, F. R.; Ashbrook, S. E.; Bühl, M.; Kilian, P.; Slawin, A. M. Z.; Woollins, J. D. *Organometallics*, **2014**, *33*, 2424.

(33) Athukorala Arachchige, K. S.; Sanz Camacho, P.; Ray, M. J.; Chalmers, B. A.; Knight, F. R.; Ashbrook, S. E.; Bühl, M.; Kilian, P.; Slawin, A. M. Z.; Woollins, J. D. *Organometallics*, **2014**, *33*, 2424.

(34) Hupf, E.; Lork, E.; Mebs, S.; Beckmann, J. *Organometallics*, **2014**, *33*, 2409.

(35) Davies, A. G., Organotin Chemistry; Wiley-VCH: Weinheim, Germany, 2004.

(36) Carrera, N.; Pérez-Temprano, M. H.; Albéniz, A. C.; Casares, J. A.; Espinet, P. *Organometallics*, **2009**, *28*, 3957.

(37) Nagy, P.; Szabó, D.; Kapovits, I.; Kucsman, Á.; Argay, G.; Kálmán, A. *J. Mol. Struct. (THEOCHEM)* **2002**, *606*, 61.

(38) (a) Roesky, H. W.; Andruh, M. *Coord. Chem. Rev*. **2003**, *236*, 91. (b) Koizumi, T.; Tsutsui, K.; Tanaka, K. Eur. J. Org. Chem. 2003, 4528. (c) Janiak, C. *J. Chem. Soc. Dalton Trans*. **2000**, 3885.

(39) (a) Nishio, M. *CrystEngComm.* **2004**, *6*, 130; Fischer, C.; Gruber, T.; Seichter, W.; Schindler, D.; Weber, E. *Acta Crystallogr., Sec. E* **2008**, *E64*, o673. (b) Hirota, M.; Sakaibara, K.; Suezawa, H.; Yuzuri, T.; Ankai, E.; Nishio, M. *J. Phys. Org. Chem.* **2000**, *13*, 620. (c) Tsubaki, H.; Tohyama, S.; Koike, K.; Saitoh, H.; Ishitani, O. *Dalton Trans.* **2005**, 385.

(40) (a) Balas, V. I.; Banti, C. N.; Kourkoumelis, N.; Hadjikakou, S. K.; Geromichalos, G. D.; Sahpazidou, D.; Male, L.; Hursthouse, M. B.; Bednarz, B.; Kubicki, M.; Charalabopoulos, K.; Hadjiliadis, N. *Aust. J. Chem*. **2012**, *65*, 1625. (b) Greene, P. T.; Bryan, R. F. *J. Chem. Soc. A* **1971**, 2549. (c) Davies, A. G.; Milledge, H. J.; Puxley, D. C.; Smith, P. J. *J. Chem. Soc. A* **1970**, 2862. (d) Sawyer, J. F. *Acta Crystallogr., Sect.C: Cryst. Struct. Commun.* **1988**, *44*, 633.

(41) CrystalClear 1.6; Rigaku Corp., 1999. CrystalClear Software User's Guide; Molecular Structure Corp., The Woodlands, TX, 2000. Flugrath, J. W. P. *Acta Crystallogr., Sect. D* **1999**, *D55*, 1718.

(42) SIR97: Altomare, A.; Burla, M.; Camalli, M.; Cascarano, G.; Giacovazzo, C.; Guagliardi, A.; Moliterni, A.; Polidori, G.; Spagna, R. *J. Appl. Crystallogr*. **1999**, *32*, 115.

(43) DIRDIF99: Beurskens, P. T.; Admiraal, G.; Beurskens, G.; Bosman, W. P.; de Gelder, R.; Israel, R.; Smits, J. M. M. The DIRDIF-99 program system; Technical Report of the Crystallography Laboratory, University of Nijmegen, Nijmegen, The Netherlands, 1999.

(44) CrystalStructure 3.8.1: Crystal Structure Analysis Package; Rigaku and Rigaku/MSC, 9009 New Trails Dr., The Woodlands, TX 77381, USA, 2000−2006.

(45) SHELX97: Sheldrick, G. M. *Acta Crystallogr., Sect. A* **2008**, *64*, 112.

Authors are required to submit a graphic entry for the Table of Contents (TOC) that, in conjunction with the manuscript title, should give the reader a representative idea of one of the following: A key structure, reaction, equation, concept, or theorem, etc., that is discussed in the manuscript. Consult the journal's Instructions for Authors for TOC graphic specifications.